Chapter 3
The Measurements of the Oxygen Reduction Reaction

Juhong Cheng, Xiaojun Lin, and Pei Kang Shen

Abstract The oxygen reduction reaction is a typical electrocatalytic reaction, which is very sensitive to the surface state of the electrode and the type of adsorbate, and is the object of many basic researches. In this chapter, we mainly start from the oxygen reduction reaction mechanism, discuss the measurement technology of the oxygen reduction reaction in detail, discuss the key techniques for obtaining the oxygen reduction polarization curve, and analyze the experimental data.

Keywords Oxygen reduction reaction · Cyclic voltammetry · Rotating ring disk electrode · Reference electrode · Working electrode · Electrochemical specific surface area

3.1 Oxygen Reduction Reaction Mechanism and Testing Method

As described in 1.2.2, the kinetics of the oxygen reduction reaction limits the overall performance of the fuel cell. In addition, this reaction also plays an important role in the corrosion system. Oxygen reduction is also a typical electrocatalytic reaction, sensitive to the surface state of the electrode and the type of adsorbate, so it is also the object of many basic researches. These basic researches focus on the effects of different electrode materials, crystal faces, surface atom modifications, electrolyte types, and contaminating ions on reaction kinetics and reaction progress.

J. Cheng
Hunan Aerospace TianLu Advanced Matirial Testing Co., Ltd., Ningxiang High-Tech Zone, Changsha, China

X. Lin
Southern University of Science and Technology, Shenzhen, Guangdong, China

P. K. Shen (✉)
Collaborative Innovation Center of Sustainable Energy Materials, Guangxi Key Laboratory of Electrochemical Energy Materials, College of Chemistry and Chemical Engineering, Guangxi University, Nanning, Guangxi 530004, China
e-mail: pkshen@gxu.edu.cn

P. K. Shen, *Electrochemical Oxygen Reduction*,
https://doi.org/10.1007/978-981-33-6077-8_3

Research on the electrochemical behavior of oxygen has been around for a long time, and there are many research teams and review articles. Although the reduction of molecular oxygen is a crucial step, the oxygen reduction reaction is an extremely complex four-electron reaction, and unstable intermediates are easily formed in the reaction, such as hydrogen peroxide generation by two-electron reaction (H_2O_2), thereby reducing energy conversion efficiency. The intermediate, H_2O_2, will damage the membrane in fuel cells by combining transition metal cations, like iron ion, to proceed with a Fenton reaction as follows.

$$M^{2+} + H_2O_2 \rightarrow M^{3+} + {}^{\bullet}OH + OH^- \tag{3.1}$$

$$M^{3+} + H_2O_2 \rightarrow M^{2+} + {}^{\bullet}OOH + H^+ \tag{3.2}$$

where M^{2+} is the transition metal cation. These metal ions will react with hydrogen peroxide and produce-free radicals to attack the weak sites in a membrane. In a perfluorinated sulfonic acid membrane electrode, the weak polymer end groups or the side chain cleavage are the potential sources of carboxylic acid end groups. Once the carboxylic acid end groups are formed, it will be attacked by free radicals in an unzipping reaction:

$$\sim CF_2COOH + 2OH^- \rightarrow COOH + CO_2 + 2HF \tag{3.3}$$

If the structure of the membrane is damaged, the pinhole formation, fragmentation and short circuit of the system become possible. The following is a brief introduction to the common reaction mechanism of oxygen reduction in fuel cell systems.

3.1.1 Oxygen Reduction Reaction Mechanism

In the acidic solution, the total reaction formula of the four-electron reaction in which oxygen is reduced to water is expressed as follows.

$$O_2 + 4H^+ + 4e^- \rightarrow 2H_2OE = 1.229\ \text{V}\ vs.\ \text{SHE}25\,^{\circ}\text{C} \tag{3.4}$$

The overall reaction equation in an alkaline solution is,

$$O_2 + 2H_2O + 4e^- \rightarrow 4OH^-E = 0.40\ \text{V}\ vs.\ \text{SHE}25\,^{\circ}\text{C} \tag{3.5}$$

1.229 and 0.40 V are theoretical equilibrium potentials, calculated from thermodynamic data.

The Gibbs free energy generated by the standard mole of 1 mol of liquid water is −237.142 kJ mol^{-1}, the Faraday constant is 96485 C mol^{-1}, the number of transferred electrons is 2, and the conversion formula of Gibbs free energy and electrode potential is obtained.

$$E = -\frac{\Delta G}{\mathrm{nF}} \tag{3.6}$$

It can be calculated that the theoretical equilibrium potential for generating 1 mol of liquid water at 298 K is 1.229 V. It can be seen from the Gibbs free energy of this reaction that the reaction is thermodynamically spontaneous, but because the reaction rate is extremely slow and limited by the reaction kinetics, an external catalyst is needed to improve its kinetics performance.

In addition, the entire process of this reaction involves many intermediates, electron transfer processes, and reaction steps. Figure 3.1 shows the chemical potential of different oxygen reduction intermediates in an acidic solution. As can be seen from this figure, there are many possible reaction processes during the reaction, but the actual situation is much more complicated than that described in this figure, because different intermediates will interact with the electrode surface, including the intermediate product adsorbed on the surface of the electrode, the surrounding adsorbed material, and the ions in the electrolyte solution, etc., so the chemical potential of the intermediate product is affected by the system test conditions. At present, the simplification steps of the oxygen reduction reaction approved by most research teams are direct four-electron reaction and indirect two-electron reaction. The difference between the two is whether there is an intermediate product hydrogen peroxide. As seen in Fig. 3.1, the direct four-electron reaction requires the surface of the electrode

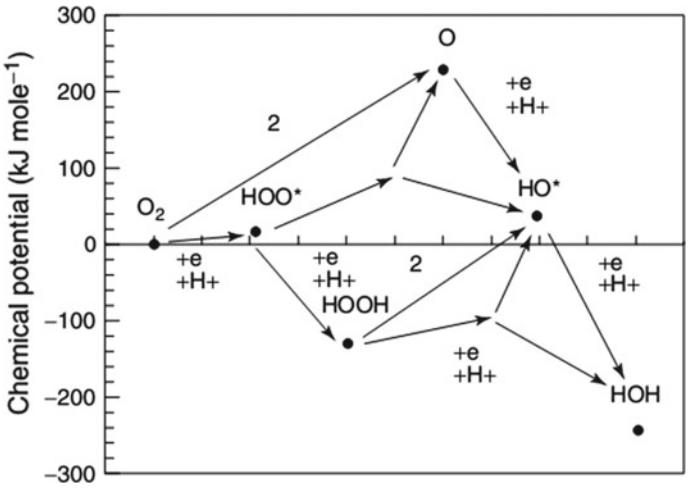

Fig. 3.1 Chemical potential of different oxygen reduction intermediates in an acidic solution

to have a chemical potential for the complete reduction of the intermediate species, which can only be achieved on a few metal surfaces, such as the (100) crystal planes of platinum, palladium, silver and gold. Most materials, including carbon, mercury, other crystal faces of gold, and oxide-modified metals, are indirect two-electron reactions. The direct four-electron reaction and indirect two-electron reaction in acidic and alkaline solutions are briefly described below.

In an acidic aqueous solution, the reduction reaction of oxygen on a metal such as platinum is carried out by a direct four-electron reaction, taking metal Pt as an example, that is,

$$2Pt + O_2 \rightarrow 2Pt\text{-}O \tag{3.7}$$

$$2Pt\text{-}O + 2H^+ + 2e^- \rightarrow 2Pt\text{-}OH \tag{3.8}$$

$$2Pt\text{-}OH + 2H^+ + 2e^- \rightarrow Pt + 2H_2O \tag{3.9}$$

The overall response is still of formula (3.4).

In addition, if the oxygen molecule is reduced by an indirect two-electron reaction, two electrons are reduced to H_2O_2.

$$O_2 + 2H^+ + 2e^- \rightarrow H_2O_2 E = 0.68\ \text{V}\ (vs.\ \text{SHE}\ 25\ ^\circ\text{C}) \tag{3.10}$$

Due to the instability of the intermediate H_2O_2, the catalytic decomposition reaction is easily carried out and further reduced to water.

$$H_2O_2 + 2H^+ + 2e^- \rightarrow 2H_2O \quad E = 1.78\ \text{V}(vs.\ \text{SHE}\ 25\ ^\circ\text{C}) \tag{3.11}$$

The process (3.11) also yields two electrons, but the potential of the reaction is much higher than the process (3.4), resulting in increased energy consumption for energy conversion. From the perspective of output voltage and energy conversion, the number of electron transfer in the four-electron process is double that of the two-electron process, that is, the energy is converted to twice. This is why oxygen reduction is a direct four-electron process. Especially in the energy conversion process, the four-electron oxygen reduction reaction is a requirement for maximizing energy conversion.

In an alkaline solution, the reaction mechanism of O_2 can generally be expressed as follows.

If O_2 is directly reacted to water by direct four-electron processes, the total reaction equation is as shown in (3.4); if an indirect two-electron process occurs, the following processes may occur.

O_2 first occurs in a single electron reaction to generate O_2^-

$$O_2 + e^- \rightarrow O_2^- \tag{3.12}$$

O_2^- is protonated to HO_2^- by a water molecule, which is also a single electron reaction.

$$O_2^- + H_2O \rightarrow HO_2^- + OH \tag{3.13}$$

$$OH + e^- \rightarrow OH^- \tag{3.14}$$

Then the total response of the two-electronic processes is.

$$O_2 + H_2O + 2e^- \rightarrow HO_{2-} + OH^- \tag{3.15}$$

HO_{2-} formed by two electron processes through O_2 has two further reaction pathways.

The first is catalytic decomposition of the electrode surface to adsorbed oxygen.

$$2HO_2^- \rightarrow 2OH^- + O_2 \tag{3.16}$$

The second is electrochemical reduction to OH^-.

$$HO_2^- + H_2O + 2e^- \rightarrow 3OH^- \tag{3.17}$$

In fuel cells, in order to obtain maximum output power and reduce corrosion of carbon carriers or other materials due to peroxides, optimization studies of oxygen reduction catalysts are directed to achieving a direct four-electron reaction of the catalyst. The two-electron reaction is mainly used to study the preparation of hydrogen peroxide.

3.1.2 Oxygen Reduction Reaction Test Means

The current techniques for studying the state of adsorption of particles on metal surfaces are basically not used to detect the mechanism of oxygen reduction in situ, mainly because these techniques basically require working under ultra-high vacuum conditions, but almost no electrochemical system is capable of working under vacuum. For example, electron or optoelectronic-based technologies, including EELS, AES, XPS, and UPS, cannot be used in situ to determine electrode reactions because the electrolyte solution will volatilize. Similarly, TPD also requires work to test the desorption of adsorbate under vacuum conditions. Infrared Reflectance Absorption Spectroscopy (IRAS) can be used for in situ testing, but the oxygen stretching IR cross-section is too small and the strong adsorption of the electrolyte

makes this test technique difficult to perform accurate analysis. X-ray absorption spectroscopy techniques such as extended X-ray absorption fine structure spectroscopy (EXAFS) and near-edge X-ray absorbing fine structure spectroscopy (NEXAFS) can also be used for oxygen reduction mechanism studies, but the information about the reaction mechanism that can be obtained is very limited [1–4]. Strasser et al. used Synchrotron radiation X-ray diffraction to study the structural properties of PtCo particles [5, 6]. Wieckowski et al. improved the NMR method to make it suitable for electrochemical working conditions, and used this method to study the oxygen reduction reaction [7].

The earliest mechanism for studying the mechanism of oxygen reduction in situ is the fixed electrode method proposed by Damjanovic et al., but the fixed electrode method was greatly affected by the mass transfer of the solution. The current in situ study of oxygen reduction kinetics mainly uses the rotating disk electrode method (see 3.2.2 for detailed analysis). Rotating disk electrode is a fluid dynamic electrode that increases liquid flow by convection and improves mass transfer. This electrode can be used to study the progress of electrochemical reactions in steady state, transient, constant voltage or constant current conditions. The voltage and current data obtained by rotating the disk electrode are plotted as a Koutecký-Levich curve with the reciprocal of the current and the reciprocal of the square of the electrode speed, the intercept of the curve is the limiting current density. The limiting current density is proportional to the electrochemical reaction rate and can therefore be used to compare the kinetic mechanisms of different reactions. Since the rotating disk electrode cannot obtain the information of the oxygen reduction reaction intermediate product, a rotating ring disk electrode has been researched on the basis of the rotating disk electrode for studying the intermediate products in the reaction process, such as H_2O_2in the oxygen reduction reaction. And this method is used to study the factors affecting oxygen reduction, such as the influence of different electrolyte solutions, including H_3PO_4, H_2SO_4, $HClO_4$, trifluoromethanesulfonic acid (TFMSA) and the like. In addition, the commonly used catalyst active material platinum and the proton membrane Nafion for PEMFC were slurried to form a catalyst electrode for oxidative kinetics studies.

3.2 Research Method of Electrochemical Oxygen Reduction Reaction

3.2.1 Cyclic Voltammetry

There are many experimental methods for testing the polarization curves of electrochemical systems. According to the types of independent variables, they can be simply divided into constant current method (control current method) and constant potential method (control potential method). The constant current method records the change relationship (polarization curve) between the corresponding electrode

potential and current density by controlling a given current density. The apparatus used in this method is simple and easy to control, but is not suitable for electrodes that vary greatly in current density or electrode surface state. The constant potential method is a technique for controlling the potential of a given electrode and measuring the relationship between the potential of the electrode and the current density. It is also the most widely used method.

According to the relationship between electrode process and time, the test method can be divided into steady-state method and transient method. The steady-state method means the current potential curve of the measuring electrode in a steady state, in this case, the current density and the electrode potential are independent of time and do not change with time. The transient method is a curve showing the current potential change of the electrode process when the steady state is not reached, and the influence of the time factor on the electrode reaction is considered. The following mainly introduces the basic working principle of the constant potential method for measuring cyclic voltammetry.

The first use of cyclic voltammetry for scientific research dates back to about 80 years ago—Electrochemical studies by Heyrovsky et al. In their research, linear scanning and cyclic voltammetry have been used for polarographic analysis. The working electrode of this test is mercury, the counter electrode and the reference electrode are both large-area calomel electrodes, and the potential region of interest is negative compared with the calomel electrode, so the cyclic voltammetry curve appears in the first quadrant. The study did not use the mathematical analysis of reversible and irreversible reaction electron transfer proposed by Matsuda and Ayabe in 1955 to determine the positive sweep potential. Moreover, there is no electronic potentiostat (invented in 1954), and the calomel electrode serves as both the counter electrode and the reference electrode, so it is necessary to correct the voltage drop caused by the solution resistance between the working electrode and the calomel electrode. After extensive application of potentiostats, cyclic voltammetry and linear voltammetry began to be applied to the three-electrode test system (Fig. 3.2). The

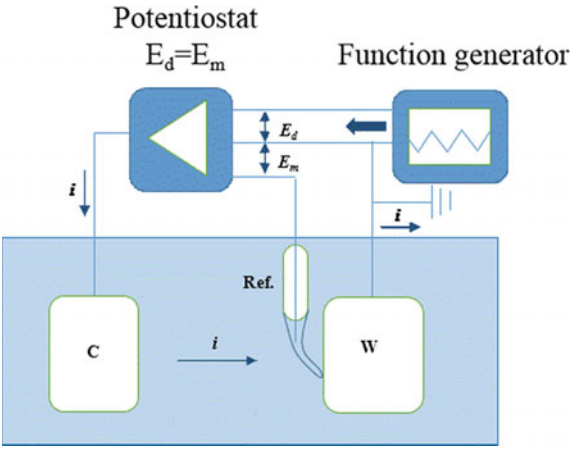

Fig. 3.2 Basic circuit diagram of the potentiostat. (W, C, and Ref. are the working electrode, the counter electrode, and the reference electrode, respectively; Ed is the driving potential difference, and Em is the test potential difference)

electrode potential can be controlled by applying a driving potential difference Ed between the reference electrode and the working electrode. In addition, by adding the Luggin capillary and shortening the distance between the Luggin capillary and the working electrode, most electrochemical tests do not require solution resistance correction for iR drop. Therefore, this potential scanning technique is applicable to most metal electrodes. Moreover, the scanning rate and the potential scanning interval of the cyclic voltammetry curve are controlled, and the electrochemical process of the metal or alloy surface is highly reproducible. Today, this potential scanning method has been widely used in the research of various electrode processes.

Figure 3.2 shows a simplified potentiostat test circuit. The most important electronic device is the potential comparison circuit, which has the following two functions. The first is to make the control potential Ed (obtainable by the function generator) equal to the effective potential difference Em between the working electrode and the reference electrode. Since the response times of the balanced potentials, Ed and Em are in the order of microseconds, the input voltage allowed by the output current can oscillate beyond 10 kHz. Another function is to convert the current signal between the working electrode and the counter electrode into a voltage signal through a resistor R. In order to ensure that the output current signal is only from the counter electrode and the working electrode, the reference electrode needs to be connected to a very high resistance R. The voltage drop of the resistor R and the potential Ed are plotted as images by an x/y recorder or as digital signals.

The potentiostat has three interfaces that can be connected to the working electrode, the reference electrode and the counter electrode. Therefore, as long as an external fixed resistor is used, the potentiostat can also be used for constant current testing. The working electrode and the reference electrode are disconnected from the potentiostat, and the input terminals of the potentiostat are connected to the fixed resistor Rg. Then, the input terminal of the reference electrode is connected to the working electrode, and the potential of the working electrode is referenced by the reference electrode. If the output potential of the constant voltage meter is Ed, the current flowing through the working electrode will be Ed/Rg. The potential on the working electrode is changed by controlling this current. Both the galvanostatic method and the potentiostatic method can be used to test the current potential curve of a specified potential region. However, for an electrode reaction with a negative resistance value (voltage increase current decreases), stabilizing one current value may result in two voltage values and two oscillations at the same time.

In a cyclic voltammetric scan, the scan rate changes the scan direction at a set reversal point. The generally selected reversal point can present the oxidation and reduction reactions that may occur in the electrode process on the scan curves in different directions, such as the oxygen process in the forward scan and the hydrogen process in the negative scan. The linear scan curve is a one-way (forward or negative) sweep volt-ampere curve over a specified potential interval. For the surface reaction process of most metals or alloys, when the scanning rate is 50–500 mVs^{-1}, the surface state of the metal or alloy is basically unchanged after undergoing a complete cyclic voltammetry scanning process, thus ensuring the test repeatability. Platinum, gold and palladium, the test results are highly reproducible. Electrochemical testing of

other electrode materials is very sensitive to the purity of the electrolyte solution. When the sweep speed is lower than 5–10 mV s^{-1}, the surface is prone to passivation. In the case of rapid scanning, impurities adsorbed on the surface may be removed by oxidation or reduction, but may also cause the electrode reaction of interest to be suppressed.

3.2.2 Rotating Circular (Ring) Disk Electrode

3.2.2.1 Rotating Circle (Ring) Disk Electrode Overview

Molecular oxygen reduction reaction is usually measured by the rotating disk electrode (RDE) or the rotating ring-disk electrode (RRDE) which is an inimitable electrode system that can give a quantitative analysis by solving the fluid dynamics and convective diffusion equation.

It has long been observed that in the stirred solution, there is a limiting current and a diffusion current of the steady state polarization curve. The current of the fixed electrode in the agitated state measured by cyclic voltammetry is much larger than that observed in the natural convection state and is less affected by the potential scanning speed. However, to keep the convection state constant, it is difficult to achieve by simply stirring the solution. In contrast, the electrode rotates to stabilize the convective mass transfer on the electrode surface. As early as 1900s, Nernst et al. used the rotating electrode to determine the current–potential curves of the reduction reactions of elements such as sulfur, bromine and so on, but they did not realize the importance of the electrode shape. Moreover, Kolthoff et al. did many electrochemical studies with a rotating cylindrical electrode but just putting a Pt wire into the glass tube. However, it is very difficult to analyze the current values in those reactions carried out in a rotating cylindrical electrode, because the fluid flow on the electrode surface are very complex. In 1942, Levich et al. proposed a formula for the limiting diffusion current density in a rotating disk electrode and founded a new electrochemistry system which is easier to reproduce the results and can do quantitative analysis called as rotating disk electrode system. Compared with the previous rotating electrode, its superiority is that the results can be analyzed via the calculation of fluid mechanics.

Since the flow of the solution on the rotating disk electrode is laminar, the cylindrical polar coordinate is used to solve the differential equation under steady state, and the following limit current i_d can be derived.

$$i_d = 0.62nFAD_0^{2/3}\omega^{1/2}v^{-1/6}C_0 \tag{3.18}$$

where ω is the angular velocity, v is the dynamic viscosity ($cm^2\ s^{-1}$), C_0 is the concentration ($mol{\cdot}L^{-1}$), A is the surface area (cm^2) of the electrode, and D_0 is the diffusion coefficient ($cm\ s^{-1}$).

Further deriving the above formula, the thickness of the effective diffusion layer in the liquid phase near the rotating disk electrode can be obtained.

$$\delta = 1.61 D_o^{1/2} v^{1/6} \omega^{-1/2} \tag{3.19}$$

From (3.19), we can see that the effective diffusion layer thickness δ is easy to control and calculate, and has nothing to do with the radius of the disk electrode, that is, it has the same value at every point on the surface of the disk. When the rotation speed is constant, since the state of the substance transport on the electrode is kept constant, it can obtain a stable convection state as compared with the simple solution stirring.

In addition, when the electrode reaction is reversible, the following formula holds.

$$\mathrm{E} = \mathrm{E}_{1/2} \pm \left(\frac{\mathrm{RT}}{\mathrm{nF}}\right) \ln\left(\frac{i_d - i}{i}\right) \tag{3.20}$$

Therefore, the current–potential curve is measured using a rotating disk electrode, and the reproducible data can be obtained in the same manner as the current–potential curve measured by polarographic analysis.

The nature of the current versus potential curves measured by RDEs has been derived in many electrochemistry textbooks and articles. Compared with the stationary electrode, the rotating disk electrode has the following advantages: (1) the concentration polarization is stable and the effect from concentration polarization can be eliminated to a lower degree, (2) the polarization curve is in a good stability, (3) it can be used to measure fast electrochemical reactions, (4) some important dynamic parameters such as diffusion coefficient, the number of electron transferred, the concentration of reactants and so on can be obtained by Levich equation and Koutecký-Levich equation, (5) the rate of mass transport of reactants can be controlled by adjusting the rotating rate ω, (6) incidental vibrations of RDE apparatus have little influence on the current response. Therefore, the rotating disk electrode has become an indispensable tool to study various electrochemical reactions on the electrode.

A common equation for analyzing the cyclic volt–ampere curve of a rotating disk electrode is the Levich equation [Eq. (3.18)] and the Koutecký-Levich (KL) equation as shown below.

$$\frac{1}{i} = \frac{1}{nFA_g k_f C_A} + \frac{1}{0.62nFA_g D_A^{2/3} \omega^{1/2} v^{-1/6} C_A} \tag{3.21}$$

where A_g is the geometric area of the electrode (cm^2), ω is the angular velocity (s^{-1}), v is the dynamic viscosity ($cm^2\ s^{-1}$), and k_f is the nonuniform rate constant of the electron transfer (cm s^{-1}), C_A, D_A indicates the concentration of species A (mol dm^{-3}) and diffusion coefficient ($cm^2\ s^{-1}$).

From Eq. (3.21), the plot of $1/i$ versus $1/\omega^{1/2}$ should be linear at a fixed overpotential, where the slop and intercept are proportional to the $1/n$ and $1/k_f$, respectively. Thus, the electron transferred number n and the heterogeneous rate constant k_f can be obtained. If the electrode area is $A_g = 0.2475$ cm^2, the dynamic viscosity $\upsilon = 1.009 \times 10^{-2}$ cm^2 s^{-1}, the diffusion coefficient of O_2 is $D_{02} = 1.93 \times 10^{-5}$ cm^2 s^{-1}, and the concentration of dissolved O_2 is $CO_2 = 1.26 \times 10^{-3}$ mol·L^{-1}, the electrode reaction is a four-electron reaction, and the slope value is 8.657 mA^{-1} s$^{-1/2}$.

Additionally, the reaction mechanism on the surface of electrode can be developed by using the Koutecký-Levich plots in different overpotential. The nature of $1/i$ versus $1/\omega^{1/2}$ plots in various reaction mechanisms could be found in Ref. [8]. It can predict the reaction mechanism from Koutecký-Levich plots, which is extremely significant in the development of the novel ORR catalysts. Particularly, for those new catalysts such as non-Pt catalysts, Koutecký-Levich plots provide a simple electrochemical method to study the kinetic processes.

In order to further study the intermediates of the reaction, a rotating ring disk electrode was developed. The rotating disk electrode is composed of a disc and an outer insulating layer, and the rotating ring disk electrode has a ring of rings around the periphery of the disk. The disk and the ring are insulated, and the disk or ring surrounds the center of the circle. The central axis rotates and is adjusted and measured by the rotating system (see Fig. 3.5 for its construction). The difference between the steady-state technique of the rotating ring disk electrode and the steady-state technique of the rotating disk electrode is that while measuring the polarization curve of the disk electrode, the ring electrode can be controlled at a fixed potential for detecting the generated on the disk electrode, reaction intermediate. Therefore, rotating the ring disk electrode is one of the important tools for studying or detecting the unstable intermediate products generated during the electrode process and studying the reaction mechanism of the electrode. Since two working electrodes need to be controlled simultaneously during the measurement process, the rotating ring disk electrode needs to be measured using a dual potentiostat or two potentiostats.

The rotating ring-disk electrode has the same solution flowing course as the rotating disk electrode. The bulk solution flows from the disk electrode to the ring electrode, resulting in the transmission of electrolyte which connects the ring electrode with the disk electrode so that the chemical species generated on the disk electrode can be detected on the ring electrode. For example, when there is a red body (Red) in the bulk solution, rotating up the electrode, Red will transfer from the bulk solution to the surface of disk electrode and reacts on the disk as follows.

$$\text{Red} - \text{ne-} \rightarrow \text{Ox} \tag{3.22}$$

The reduced (Ox) product produced on the disk electrode will transfer to the electrode in the direction of flowing. Therefore, if the ring electrode is fixed at a potential for Ox to be oxidized, the reaction is shown below.

$$\text{Ox} + \text{ne-} \rightarrow \text{Red'} \tag{3.23}$$

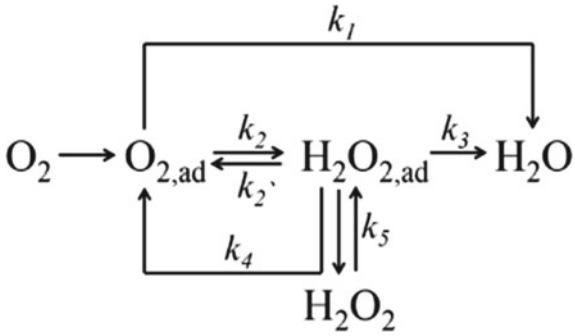

Fig. 3.3 Diagram of the oxygen reduction mechanism proposed by Damjanovic et al.

The oxidant (Ox) can be detected according to the reduction reaction formula. It can be seen that by rotating the ring disk electrode method, we can obtain information about the product or intermediate of the electrode reaction.

The mechanism of the oxygen reduction reaction is currently the most commonly used direct four-electron and indirect two-electron reactions proposed by Damjanovic et al. The mechanism diagram is shown below (Fig. 3.3).

The oxygen molecules adsorbed on the surface of the electrode can directly form water by a four-electron process (rate constant k_1), or H_2O_2 can be generated by a two-electron reduction reaction (rate constant k_2). The H_2O_2 produced can be reduced to water (rate constant k_3), either directly desorbed (rate constant k_5) or oxidized to oxygen molecules (rate constant k_2'). In addition, a part of H_2O_2 can participate in the catalytic reaction of the electrode and further catalytic decomposition (rate constant k_4). This complex process provides a thorough analysis with rotating ring disk electrodes. Reference [9] details how the oxygen reduction mechanism is analyzed by the relationship between the ring current and the disk current and the rotational speed. From the usual considerations, the following additional conditions are introduced to illustrate how to determine the rate constant of each reaction step of oxygen reduction by ring current, disk current and rotation speed.

If an oxygen reduction reaction occurs on the disk electrode and the oxidation potential of H_2O_2 is set to a potential for diffusion control, it is assumed that all reactions are first-order reactions, and O_2 and H_2O_2 are in adsorption–desorption equilibrium. Then, the relationship between the ring current I_R and the disk current I_D can be expressed by the following two equations.

$$\frac{I_D}{I_R} = \frac{1}{N}\left\{\frac{2k_1 + k_2}{k_2} + \left[\frac{(2k_1 + k_2)(k_3 + k_2' + k_4)}{k_2} + (k_3 - k_2')\right]\frac{r_{H_2O_2}}{D_{H_2O_2}\sqrt{\omega}}\right\} \tag{3.24}$$

$$\frac{I_{dO_2} - I_D}{I_R} = \frac{1}{N}\left\{1 + 2\frac{(k_1 + k_2' + k_4)}{k_2}\frac{D_{O_2} r_{H_2O_2}}{D_{H_2O_2} r_{O_2}} + \frac{2D_{O_2}\sqrt{\omega}}{k_2 r_{O_2}}\right\} \tag{3.25}$$

In the formula $I_{d\ O_2} = 4Fr_{O_2}C\sqrt{\omega}$, is the limiting current of the four-electron reaction of oxygen molecules, r = 0.62D2/3v−1/6, D is the diffusion coefficient, v is the dynamic viscosity coefficient, and ω is the electrode rotation speed.

Taking $\frac{I_D}{I_R}$ or $\frac{I_{d\ O_2}-I_D}{I_R}$ as the X axis and ω(−1/2) as the y axis, the above two equations can be drawn as two straight lines. The two slopes and the two intercepts of the two lines can list four equations with five rate constants as variables. However, an equation is still needed to completely solve these five variables. Other additional conditions can be introduced. For example, it is assumed that the change in potential does not affect the catalytic decomposition of hydrogen peroxide (k_4), or that k_2 and $k_{2'}$ are linked by the standard equilibrium potential of the O_2/H_2O_2 pair.

Therefore, the determination steps of the oxygen reduction reaction can be studied by analyzing the ratio of the ring current to the disk current at a fixed potential, I_D/I_R, $(I_d-I_R)/I_R$, and the rotational speed ω (−1/2), and solve the rate constant for each reaction step.

3.2.2.2 Film Rotating Round (Ring) Disk Electrode

The simplest catalyst activity test method is membrane electrode test, but due to the mass transfer of the oxygen reduction reactant to the membrane electrode, the incomplete utilization of the electrocatalyst and the influence of water during the reaction, it is difficult to obtain the intrinsic electrocatalysis of the high specific surface area catalyst performance. The rotating ring (ring) disk electrode can eliminate the mass transfer effect, obtain the catalytic kinetic limit, and can quantitatively analyze the intermediate products of the reaction, and then analyze the reaction mechanism.

In 2001, the research team of Schmidt and Gasteiger proposed using a thin-film rotating disk electrode method (TF-RDE) to simulate a fuel cell membrane electrode test to study the kinetic limit of the catalyst without mass transfer and no ohmic drop. This method is based on predecessors, dating back to 1976 by Stonehart and Ross, who used a rotating thin-layer electrode (RTLE) to directly test the electrochemical rate constant of a high specific surface area catalyst. The preparation method of coating the porous catalyst on the surface of the rotating disk electrode at that time was similar to the preparation of a gas diffusion electrode of Teflon platinum thin-film electrode (PTFE). Therefore, the treatment analysis method of the rotating thin layer electrode is similar to the Teflon platinum thin-film electrode model, and is established on the full penetration model, that is, the void of the porous film layer is also sufficiently wetted. In order to explain the mass transfer efficiency of the porous catalyst layer, the model introduces an effective mass transfer coefficient Ɛ, which is the ratio of the measured current density to the net current density without any mass transfer, and is affected by the exchange current density, the diffusivity of the reactant in the porous liquid region of the porous layer, the ratio of the active material of the catalytic layer, and the thickness of the catalytic layer. For slow reaction or thin catalytic layer electrodes, the effective mass transfer coefficient Ɛ is approximately equal to 1, and the Ɛ of each region of the catalytic layer is substantially the same,

that is, the concentration of the reactants is the same whether it is the porous layer on the surface of the electrode or the internal catalytic layer. This means that the current distribution of the catalytic layer is uniform. In other words, in the complete catalytic layer, the utilization of the electron conductor and the ionic conductor can reach 100%. Conversely, for fast reaction or thick film, the effective mass transfer coefficient $\mathfrak{E}$ is close to zero, and the internal catalytic layer has almost no reactive species, resulting in a decrease in the utilization rate of the catalytic layer.

In 1987, Tanaka et al. further expanded the RTLE process and tested the oxygen reduction performance of high specific surface area catalyst Fe-phthalocyanine. They applied a slurry of catalyst and Teflon to the disk electrode cavity of a rotating disk electrode with a thickness of about 100 μm, and called this technique a porous thin-layer coating technique (TPC-RDE). Although the film resistance is large enough to affect the correctness of the test for the 100 μm film, they only use RTLE to compare the similarities and differences of several catalytic systems, and do not discuss the dynamic properties of the system, or the thickness. The effect of the film on mass transfer. Subsequently, Perez et al. used the same method to study the oxygen reduction performance of carbon-supported platinum catalysts. To explain the effect of the porous membrane catalytic layer with a thickness of 100 μm on mass transfer, they cited the PTFE full permeability model to calculate the oxygen reduction kinetic parameters. However, only about 10–50% of the catalyst solids produced by Perez et al. can be wetted, resulting in incomplete electron and ion conduction of the catalyst. Similar to the TPC-RDE model, Gloaguen et al. further reduced the thickness of the film. The thin active disk electrode layer (TAL–RDE) made of the catalyst/Nafion slurry coated on the platinum carbon rotating disk electrode was about 1–7 μm, and study the oxygen reduction performance of the Pt/C electrode to verify the effectiveness of the electrode using the full penetration model. In this model, a thin active layer can be seen as a superposition of an ionic conductor (Nafion) and an electron conductor (catalyst). This means that the solubility and diffusion coefficient of the reactants in the Nafion membrane and the solubility and diffusion coefficient of the material in the solution are fully considered. Perez et al. found that the kinetic parameters can only be obtained directly from the mass transfer correction formula in catalyst samples with a film thickness of less than 1 μm. The thicker membrane mass transfer dynamics corrections are related to the applied model and additional corrections need to be considered. Moreover, the accuracy of these kinetic parameters is affected by the accuracy of the physical property data of the catalyst/Nafion layer. However, compared to TPC-RDE, TAL-RDE is 100% wetted and all catalyst layers are involved in electron and ion conduction. In 1987, Alonso-Vante and Tributsch used a rotating thin-layer electrode to study the oxygen reduction performance of Mo4.2Ru1.8Se8 catalyst. They also deposited a mixture of catalyst/Nafion on the glassy carbon rotating disk electrode, but did not give details. Preparation information and film thickness data. Similarly, Tamizhmani, Gojkovic, Claude et al. used a similar method to study the oxygen reduction performance of different catalysts. However, their film is thicker, the ratio of Nafion to catalyst is high, and the loading of the catalyst is also large, which also leads to an increase in the material diffusion resistance of the film, which affects the correction of the dynamic current

density (mathematical simulation). Calculations and experiments have shown that the reduction in film thickness is beneficial to simplify the correction of the kinetic current).

Based on previous research results, in 2001, Paulus, Schmidt and Gasteiger proposed the film rotation (ring) disk electrode method [TF–R(R)DE]. They prepared a 20 wt % Pt/Vulcan XC 72 catalyst with Nafion as a catalyst slurry and applied it to a polished glassy carbon electrode with a loading of 28 μg Pt cm^{-2}. According to the mass of Nafion and electrode area estimates, the Nafion film thickness is about 0.1–0.2 μm. Although the film thickness is submicron, it is enough to allow the catalyst particles to adhere to the surface of the glassy carbon substrate. The optical microscope shows the catalyst/Nafion layer. The total thickness is approximately 1 μm. The cyclic voltammogram of this electrode is similar to the polycrystalline Pt electrode. In addition, if the error of the dispersion of the high-resolution lens is calculated and the error of the active area is calculated by the electrochemical method, the surface platinum concentration calculated by the hydrogen underpotential deposition method is $n_{Pt,s} = 4.2 \times 10^{-8}$ mol_{Pt} cm^{-2}, this is very close to $n_{Pt,s} = 3.7 \times 10^{-8}$ mol_{Pt} cm^{-2} calculated from the dispersion of platinum and the dispersion of the grain size of the platinum particles, which means that the utilization rate of the Pt/Vulcan catalyst is basically 100%. [10] In addition, the hydrogen desorption and desorption of different platinum-loaded catalysts are linear with the platinum loading, which also demonstrates the effectiveness of the method. The repeatability of this method was also confirmed by comparing the amount of electricity in the hydrogen desorption zone of the electrode with a platinum loading of 7 μg $_{Pt}$ cm^{-2} and 14 μg $_{Pt}$ cm^{-2}.

Further discussing the mass transfer effect of the film thickness, Lawson D. R et al. added the influence of the film impedance to the Koutecký-Levich equation, fully considering the influence of the mass transfer diffusion resistance on the experiment. The corrected formula is as follows [11].

$$\begin{aligned} \frac{1}{j} &= \frac{1}{j_k} + \frac{1}{j_d} + \frac{1}{j_f} \\ &= \frac{1}{j_k} + \frac{1}{Bc_0\omega^{1/2}} + \frac{L}{nFc_fD_f} \end{aligned} \tag{3.26}$$

where j_k and j_d are the net kinetic current density and the diffusion limit current density, respectively, j_f is the limiting current density of the Nafion membrane, B is the Levich constant, c_0 is the concentration of the reactant in the solution, and c_f is the reactant in the membrane. The concentration, D_f is the diffusion coefficient of the reactant in the film, and L is the thickness of the film. On the smooth electrode, j_f does not exist, and the measured current density is only related to j_k and j_d. If the film thickness can be reduced such that j_f is much larger than j_k and j_d, then the film resistance is negligible. Paulus et al. mapped the Koutecký-Levich curves with different platinum loadings and different film thicknesses. The KL curve intercepts and film thicknesses of different film thicknesses were plotted to obtain the Nafion

film limiting current density j_f when the Nafion film thickness was $\leq$0.3 μm. For 40 mA.cm^{-2}, when the net kinetic current is less than 4 mA.cm^{-2}, which is less than 10% of the limiting current density j_f of the Nafion membrane, its effect on the measured current is negligible. When the same calculation method calculates 333 K, the limit current density j_f of the Nafion membrane is 70 mA cm^{-2}. As long as the net kinetic current is less than 7 mA.cm^{-2}, the effect on the measured current is negligible. This also means that the maximum mass activity obtained from the experiment is 1 A.mg-1, which is very close to the maximum mass activity of the actual PEMFC. In addition, the research team verified the effectiveness of this method in hydrogen reduction and oxygen oxidation, and introduced TF-RRDE. The collection coefficient of the method and the influence of film thickness were discussed. The results show that the method is suitable for testing oxygen reduction and high reproducibility of intermediate materials, and the data deviation is within the experimental allowable range.

The TF-R(R)DE method is simple, the catalyst film is completely wetted, the participation rate of electron conduction and ion conduction is 100%, the amount of catalyst required is very small, and the current correction is simple and easy, and the kinetics of the catalyst can be directly quantitative analysis of the limits. Therefore, this method has been widely applied to the electrochemical kinetic performance analysis of catalysts since Schmidt and Gasteiger proposed and verified feasibility.

3.3 Electrochemical Reduction Test

The oxygen reduction test first requires a suitable electrolytic cell. The electrolytic cell for measuring the oxygen reduction reaction of the rotating circular (ring) disk electrode is composed of a glass tank, a working electrode, a counter electrode and a reference electrode. Here the working electrode is a rotating circular (ring) disk electrode.

3.3.1 Reference Electrode

The measurement of the oxygen reduction reaction requires a stable reference electrode, the reference electrode does not contaminate the electrolyte and itself cannot be contaminated by the electrolyte. Reference electrodes commonly used in electrochemical testing include standard hydrogen electrodes (SHE), saturated calomel electrodes (SCE), silver/silver chloride electrodes (Ag/AgCl), mercury/mercury oxide electrodes (Hg/HgO), and Reversible hydrogen electrode (RHE).

The measurement of the oxygen reduction reaction requires a stable reference electrode, which should not contaminate the electrolyte and itself should not be

contaminated by the electrolyte. Reference electrodes commonly used in electrochemical testing include standard hydrogen electrodes (SHE), saturated calomel electrodes (SCE), silver/silver chloride electrodes (Ag/AgCl), mercury/mercury oxide electrodes (Hg/HgO), and Reversible hydrogen electrode (RHE).

The standard hydrogen electrode referred to as "SHE" is a hydrogen electrode that is reversible under standard conditions. A primary standard reference electrode for measuring the hydrogen electrode potential of various reversible electrodes. The platinum-plated platinum sheet was immersed in a solution containing hydrogen ions, and a platinum-plated platinum sheet was continuously impinged with a stream of pure hydrogen, and the hydrogen gas escaped from the upper portion. The siphon and other electrodes on one side can form a battery. The following reversible electrode reactions were carried out when hydrogen was adsorbed on platinum black and contacted with an aqueous solution:

$$1/2\mathrm{H_2g} \rightleftharpoons \mathrm{H^+}\left(a_{\mathrm{H}}^{+}\right) + \mathrm{e^-} \tag{3.27}$$

According to the Nernst equation, the electrode potential (E_{H^+}/H_2) is related to hydrogen ion activity (a_{H^+}), hydrogen pressure, temperature, etc.

$$E_{H^+,H_2} = E^{\theta}_{H^+,H_2} + \frac{RT}{F}\log\frac{\mathrm{a}_{H^+}}{(P_{H_2})^{1/2}} \tag{3.28}$$

If the temperature is constant, $a_{\mathrm{H}}{}^{+} = 1$, $P_{H_2}\mathrm{P_{H2}} = 101.325$ Pa, specify the electrode potential of the hydrogen electrode

$$E_{\mathrm{H^+,H_2}} = 0$$

This electrode is then referred to as a "standard hydrogen electrode." The hydrogen electrode is very sensitive when it is applied. To obtain a stable electrode potential, it must meet strict experimental conditions. The reversible hydrogen electrode is derived from a standard hydrogen electrode, the difference being that the electrolyte solution of the reversible hydrogen electrode is identical to the electrolyte solution of the test system.

If a silver chloride is plated on the silver wire and then immersed in a solution of chloride, it is a silver–silver chloride electrode. Ag–AgCl electrode structure system is Ag | AgCl(s) | KCl, the electrode reaction is.

$$\mathrm{AgCl\ (s)} + \mathrm{e^-} \rightleftharpoons \mathrm{Ag(s)} + \mathrm{Cl^-(l)} \tag{3.29}$$

Like the calomel electrode, the electrode potential depends on the chloride ion activity in the solution, i.e.,

$$E = E^{\theta}_{\mathrm{Ag/AgCl}} - \frac{2.303RT}{F}\log \mathrm{a}_{Cl^-} \tag{3.30}$$

The detailed preparation method of the Ag/AgCl electrode is a thermal decomposition method and an electroplating method, wherein the electroplating method is simple, and the process is as follows: First, the silver wire is taken and the surface oil is first washed with acetone, and if silver is plated on the silver wire, it is required first elute with ammonia water and then rinse carefully with distilled water. Then, the silver electrode was used as the anode, the platinum wire was used as the cathode, and a layer of silver chloride was electroplated in a 1 mol·L^{-1} hydrochloric acid solution for 30 min (current density of 2 mA.cm^{-2}), and finally rinsed with distilled water. The electrode produced is purple-brown and this electrode can be applied directly without a liquid junction.

If platinum wire is used as the substrate, silver plating should first be applied to the platinum wire. Platinum wire silver plating method: First, prepare a silver plating solution ($AgNO_3$ 3 g, KCl 60 g, concentrated ammonia water 7 mL, add water to make 100 mL solution), then a platinum wire to be plated as a cathode, another platinum wire as an anode, and a series of about 2000 Ω variable resistor, voltage is set to 4 V, electroplate at 0.5 mA.cm^{-2} current density for 0.5 h. Wash the silver-plated electrode and then plate a layer of silver chloride in the same manner as above.

In 0.1 mol·L^{-1} KCl solution, the electrode potential of Ag/AgCl electrode is equal to 0.2880 V (SHE, 25 °C). The electrode potential of silver–silver chloride electrode is stable, reproducible, simple in structure and convenient to use. It is also relatively stable in seawater, so it is widely used for ship cathodic protection in addition to its application in the laboratory.

The calomel electrode is one of the most widely used reference electrodes in the laboratory. It consists of metallic mercury and mercurous chloride (Hg_2Cl_2) and potassium chloride solution.

Hg | Hg_2Cl_2 (saturated), KCl (X mol·$L^{-1)}$ (X represents the molar concentration of KCl in solution.)

$$\mathrm{HgCls} + 2\,\mathrm{e}^- \rightleftharpoons 2\mathrm{Hgl} + 2\,\mathrm{Cl}^- \tag{3.31}$$

$$E = E^{\theta}_{\mathrm{Hg_2Cl_2/Hg}} - \frac{2.303RT}{F} \log a_{\mathrm{Cl}^-} \tag{3.32}$$

A platinum wire is sealed in the inner glass tube, the platinum wire is inserted into pure mercury (thickness 0.5 to 1 cm), a paste of mercurous chloride and mercury is placed underneath, and potassium chloride is placed in the outer glass tube. The solution constitutes the calomel electrode. The contact portion of the lower end of the electrode with the solution to be tested is a porous substance such as a sintered ceramic core or a glass sand core or a capillary channel. When the temperature is fixed, the electrode potential of the calomel electrode is determined by the chloride ion activity. When the chloride ion activity is constant, the electrode potential is also constant, regardless of the pH of the solution to be tested. Different concentrations of potassium chloride solution can make its potential have different constant values. At 25 °C, different concentrations of potassium chloride solution can have different potentials

Table 3.1 Calomel electrode potential corresponding to different concentrations of potassium chloride solution (SHE, 25 °C)

KCl solution concentration ($mol \cdot L^{-1}$)	0.1	1.0	4.2 (saturation solution)
Electrode potential (V)	+0.3365	+0.2828	+0.2438

for their potentials. At 25 °C, the electrode potentials of the calomel electrodes of different concentrations of potassium chloride solution are based on standard hydrogen electrodes as follows (Table 3.1).

The saturated calomel electrode is very stable, easy to prepare and store, and easy to use. However, the results obtained with 0.1 or 1.0 $mol \cdot L^{-1}$ calomel electrodes are better. Because they can reach equilibrium potential quickly, and their potential is less dependent on temperature change, while the saturated reference electrode is affected by temperature. Larger.

The mercury–mercury oxide electrode is a commonly used reference electrode for alkaline solution systems. The electrode reaction is.

$$HgO + H_2O + 2\,e^- \rightleftharpoons Hg + 2\,OH^- \tag{3.33}$$

The standard electrode potential is 0.1100 V.

When using a standard hydrogen electrode, a saturated calomel electrode or a silver/silver chloride electrode as the reference electrode, the system needs to be pH corrected and temperature corrected because the standard electrode potential is specified at a certain temperature and pH. In a strong electrolyte solution, for every 1 pH increase, the potential should move 59 mV in the negative direction. For example, the measurement range set for an acidic solution (pH = 0) is 0–1 V (potential difference is 1 V). When the pH is 7, the measurement range should be corrected to −0.413–0.587 V. Only with such correction can the desired curve appear in the measurement range. The potential of the reference electrode is typically measured at 25 °C. When the temperature changes, temperature correction is also performed. The temperature correction formula is as follows (in the case of SHE),

$$E_{SHE,T\neq 298K} = E_{SHE,298K} + (T - 298)\left(\frac{\partial E}{\partial T}\right)_P \tag{3.34}$$

In the above formula, $E_{SHE,298}$ K is the electrode potential at 298 K or the standard electrode potential of the electrode, and $E_{SHE,T\neq 298}$ K is the electrode potential at the actual test temperature.$\left(\frac{\partial E}{\partial T}\right)_P$ is a temperature gradient at constant pressure and can be obtained from the electrochemical manual or reference electrode instructions.

In addition, if the working electrode is a Pt electrode and the reference electrode is a chloride ion electrode such as a saturated calomel electrode (SCE), a salt bridge is required. Because the chloride ions diffused into the solution are highly adsorbed on the Pt electrode, thereby affecting the oxygen reduction performance of the Pt electrode. However, when the test period is long, the salt bridge cannot effectively

prevent the chloride ions on the reference electrode from diffusing to the test electrode. Mayrhofer et al. used an ion-conducting membrane (Nafion®) instead of a salt bridge to study the effect of a saturated calomel electrode on the oxygen reduction of a platinum electrode after using an ion-conducting membrane. The results show that the oxygen reduction test is stable for up to 290 min using a system of three conductive films, independent of free chloride ions. The Nafion® ion-conducting membrane consists of a polytetrafluoroethylene skeleton and a side chain containing a sulfonate group. The sulfonate group is hydrophilic, and the polytetrafluoroethylene skeleton is hydrophobic, and the membrane allows water and cations to diffuse through. It rejects negative ions that are electrically equivalent to sulfate groups, such as chlorine, thereby preventing the passage of chloride ions.

If a reversible hydrogen electrode (RHE) is used as the reference electrode (see the U-shaped portion of Fig. 3.4), it is convenient to use. The solution in the reference electrode is the same as the test system, so pH calibration and temperature correction are not required. The measurement range of the instrument does not need to be changed regardless of the pH of the test solution. Moreover, since the electrolyte solution of the reversible hydrogen electrode is identical to the electrolyte solution of the electrolytic cell, the reference electrode does not introduce chloride ions, so there is no problem that the chloride ions contaminate the electrode, so that it is not necessary to use a salt bridge or a barrier film, so that the measurement system is simple.

The reversible hydrogen electrode can be prepared on site to ensure the purity and freshness of the electrode system. Figure 3.4 shows the electrolytic cell and reference electrode we designed. In Fig. 3.4, A and B are electrodes, C is a piston, D is a fixed (oxygen) inlet, E is a socket for the counter electrode, G is opened for insertion

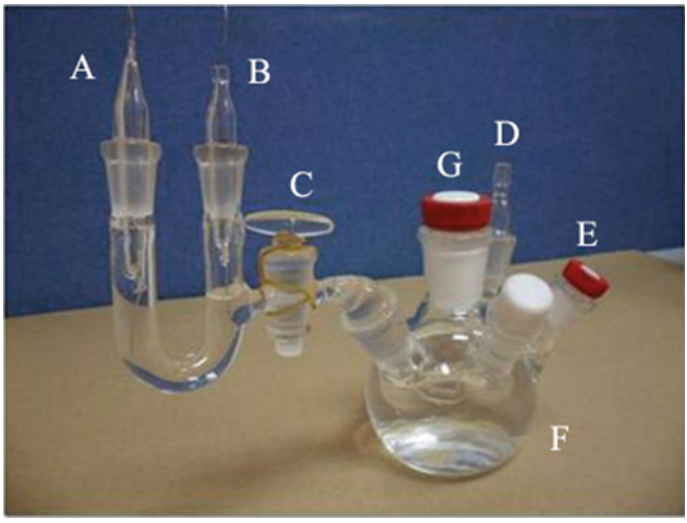

Fig. 3.4 Electrolyzer and reference electrode for rotating the ring electrode

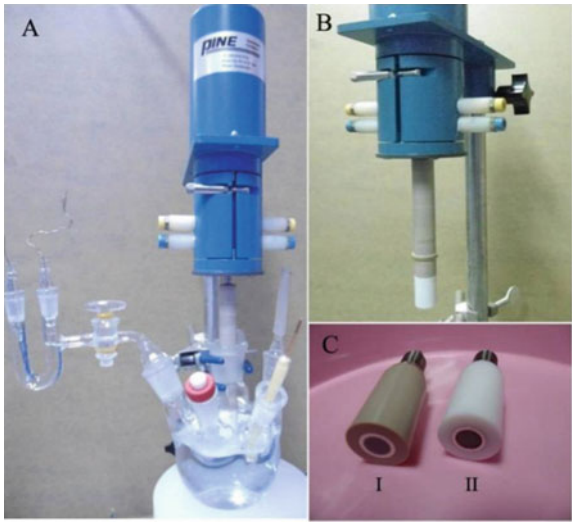

Fig. 3.5 Rotating ring disk electrode assembly. **a** Rotating ring disk electrode integral device, **b** Research electrode and rotating shaft connection and **c** Rotating ring disk electrode

into the working electrode, and F is the main body of the electrolytic cell storage liquid. According to this design, the piston C is first opened during use, and the same solution as the electrolyte solution in the electrolytic cell is filled with the reference electrode glass tubes A and B to communicate with the solution in the electrolytic cell, and then the piston C is closed in time. The two platinum or platinum black electrodes of A and B are respectively connected to a potentiostat or a regulated power supply, the positive electrode is connected to the A electrode, and the negative electrode is connected to the B electrode. Then, the electrolysis of hydrogen is started. At this time, the piston of the A electrode can be pulled apart to make the oxygen generated during the preparation run out and maintain the internal pressure balance. According to the electrochemical reaction, the electrode A generates oxygen and the electrode B generates hydrogen. When the position of the hydrogen-discharging solution produced by electrolysis is about half of the platinum electrode exposed, the electrolysis can be stopped to prevent the hydrogen from discharging the solution below the platinum electrode. Close the piston of electrode A to keep the hydrogen in a stable position. Finally, the piston C is opened, and the electrolyte in the U-tube is electrically connected to the electrolytic cell through the Lujin capillary.

Regarding the conversion between the potential of the non-RHE reference electrode and the RHE reference electrode, Gregory et al. [12, 13] calculated by the Nernst equation and the Davis equation, it is recommended to use the following conversion formula.

In 0.05 mol·L^{-1} H_2SO_4 solution.

$$E_{SHE} = E_{RHE(0.05\text{mol L}^{-1}\,H_2SO_4)} + 0.075\ \ V \tag{3.35}$$

In 0.1 mol·L^{-1} H_2SO_4 solution.

$$E_{SHE} = E_{RHE(0.1\text{mol L}^{-1}\,H_2SO_4)} + 0.060\ \text{V} \tag{3.36}$$

In 0.5 mol·L^{-1} H_2SO_4 solution.

$$E_{SHE} = E_{RHE(0.5\ \text{mol L}^{-1}\,H_2SO_4)} + 0.021\ \text{V} \tag{3.37}$$

In order to test the feasibility and rigor of the above conversion formula, we will express the detailed derivation process of the above formula as follows.

The Nernst equation of the electrode potential of the reversible hydrogen electrode can be expressed as follows.

$$E_{RHE} = E_{SHE} + \frac{RT}{F} \ln a(H^+) \tag{3.38}$$

where $\alpha(H^+)$ is the activity of H^+,$\alpha(H^+) = \frac{\gamma_+ c_+}{c^\Theta}$, γ_+ is the activity coefficient of H^+, c_+ is the molar concentration of H^+,$c^\Theta = 1$ mol·L^{-1}.

In theory, the reversible hydrogen electrode can be corrected using the Nernst equation of the hydrogen electrode. In the calculation, since γ_+ cannot be directly measured, the average activity coefficient $\gamma_\pm$ of the ions can only be measured experimentally, so in the calculation, the positive and negative ions are considered to have the same activity, and the average activity $\alpha_\pm$ is substituted for α (H^+).

When c ($H2SO_4$) = 0.1 mol·L^{-1}, the average activity coefficient $\gamma_\pm = 0.265$ [14], at 298 K.

$$\begin{aligned} E_{RHE} &= E_{SHE} + \frac{RT}{F} \ln a(H^+) \\ &= E_{SHE} + 0.0257\ \ln(0.0265 \times \sqrt[3]{4}) \\ &= E_{SHE} - 0.081\ V \end{aligned} \tag{3.39}$$

If calculated directly in molar concentration.

$$\begin{aligned} E_{RHE} &= E_{SHE} + \frac{RT}{F} \ln c(H^+) \\ &= E_{SHE} + 0.0257\ \ln 0.1 \\ &= E_{SHE} - 0.059\ V \end{aligned} \tag{3.40}$$

When c (H_2SO_4) = 0.05 mol·L^{-1}, the average activity coefficient $\gamma_\pm = 0.340$ [14], at 298 K.

$$\begin{aligned} E_{RHE} &= E_{SHE} + \frac{RT}{F} \ln a(H^+) \\ &= E_{SHE} + 0.0257\ \ln\ (0.017 \times \sqrt[3]{4}) \\ &= E_{SHE} - 0.093\ V \end{aligned} \tag{3.41}$$

If calculated directly in molar concentration.

$$\begin{aligned} E_{RHE} &= E_{SHE} + \frac{RT}{F} \ln c(H^+) \\ &= E_{SHE} + 0.0257 \ln 0.05 \\ &= E_{SHE} - 0.077\ V \end{aligned} \tag{3.42}$$

Comparing the calculated results with the conversion formula of Gregory Jerkiewicz et al., it can be found that Gregory et al. calculated the molarity directly instead of the activity, and did not perform the activity correction, so the calculation method is not rigorous. In addition, although the concentration is corrected for activity, there is a great uncertainty in the method because the activity coefficients of different solutions are difficult to measure accurately. Therefore, the general reference electrode potential and the reversible hydrogen electrode potential conversion need to know the activity coefficient at a certain acid concentration, which is actually difficult to achieve. Therefore, it can be said that it is generally not directly convertible.

Liang et al. [15, 16] recommended the use of experimental methods to convert the reference electrode potential. The reference electrode actually used in the experimental procedure was a saturated calomel electrode (SCE). When the reference electrode is corrected, the working electrode and the counter electrode of the three-electrode system are replaced with Pt wires, and the reference electrode is still a saturated calomel electrode. The electrolyte passes through high purity hydrogen to saturation. The linear scanning speed was set to 0.1 $mV.s^{-1}$, and the potential value corresponding to the current at the transition of the hydrogenation and reduction reaction was taken as the thermodynamic potential of hydrogen relative to the saturated calomel electrode. At 0.1 $mol{\cdot}L^{-1}$ $HClO_4$, the thermodynamic potential is -0.304 V, and the correction formula is $E_{RHE} = E_{SCE} + 0.304$ V; at 0.1 $mol{\cdot}L^{-1}$ KOH, the thermodynamic potential is -0.998 V, the correction formula is $E_{RHE} = E_{SCE} + 0.998$ V.

3.3.2 Working Electrode

A rotating circular (ring) disk electrode is used as the working electrode, and is composed of an outer protective material and a central disk (disc plus platinum ring) electrode. The material of the disc can be differently selected according to different testing needs. Currently, a platinum disc (platinum disc) electrode or a glassy carbon disc (platinum disc) electrode is commonly used. The platinum disk (platinum disk) electrode is relatively simple to use, only need to pay attention to the temperature and speed limit. In the study of new catalysts, in order to avoid the influence of platinum, a glassy carbon disk electrode is generally used as a base conductive material, and the surface thereof may be coated with different catalyst layers. In the following, a

glassy carbon disk (platinum disk) electrode will be taken as an example to describe the selection of the electrode and the preparation and coating of the catalyst layer.

Rotating disc (ring disc) electrodes operating under different test conditions require special manufacture. Rotating disc (ring disc) electrodes manufactured by Pine Instrument Company of the USA are of various types and are composed of different materials. The glassy carbon ring electrode used for the oxygen reduction test of the electrocatalytic system is composed of a glassy carbon disk electrode and a platinum ring electrode. Ordinary rotating ring electrodes can be used at temperatures not higher than 30 °C and rotating at speeds not higher than 3,000 rpm. The electrode working under high temperature conditions needs special production. The key point is that the electrode does not seep at high temperature. This is because the connecting wire in the electrode is a special metal material. Once the liquid is exuded, the working electrode will become the metal. Electrode, not the electrode we want to measure. Therefore, in order for the electrode to be liquid-free during operation, we need a special protective material which is equivalent to the coefficient of thermal expansion between the electrodes. Typical rotating ring electrodes manufactured by Pine Instruments of the USA are AFE6R2/GC-Pt (see Fig. 3.5(c)I) for high temperature use and AFE7R9/GC-Pt for ambient temperature (see Fig. 3.5(c)II). The insulating material at room temperature is Teflon, and the high temperature insulating material is PEEK.

The device for rotating the ring electrode is shown in Fig. 3.5. It consists of an electric rotating system, an electrolytic cell system, a constant temperature system (which maintains a constant oxygen solubility), and an electrochemical test instrument. Figure 3.5a shows the overall assembly drawing, Fig. 3.5b shows the study electrode mounting, and Fig. 3.5c shows the ring disk electrode. When using, connect the electrode to the rotating shaft Fig. 3.5b, and finally insert it into the electrolytic cell.

In the new catalyst study, when the experimental instrument is ready, the catalytic layer is prepared on the surface of the glassy carbon electrode. The following describes the method for preparing the catalytic layer in our laboratory, as follows.

First, a small amount of catalyst sample was accurately weighed by an electronic balance, dispersed in distilled water, ultrasonically shaken for 15 min, and then centrifuged for 30 min until the catalyst and moisture layers were removed, and the water was removed. This step was to clean the catalyst and reduce the influence of impurities. The catalyst was then dispersed in water/alcohol, and a certain amount of a 5% Nafion suspension solution (manufactured by DuPont, USA) was added, and ultrasonically dispersed to prepare an ink-like slurry. The slurry should be well dispersed and cannot be agglomerated or precipitated. A proper amount of slurry was accurately transferred with a 25.0 μl micro-syringe, uniformly coated on the surface of the electrode, and baked to dryness under an infrared lamp to form a uniform thin layer of catalyst on the surface of the electrode. The general usage is $10 \mu g_{Pt}$ cm^{-2}–$40\ \mu g_{Pt}\ cm^{-2}$.

It has been reported in the literature [7, 8] that the Pt/C layer with a glassy carbon surface of less than 0.1 μm does not affect the distribution of oxygen on the electrode. Intrinsically hydrophobic catalysts, as well as alcohol or high temperature treated

samples, may need to increase the ratio of alcohol (ethanol or isopropanol) to water for better dispersion. Increasing the ratio of isopropanol to water and multiple ultrasonic oscillations can obtain a slurry with a good dispersion state, thereby improving the dispersibility and electrocatalytic activity of the catalytic layer. The hydrophilic catalyst is well dispersed in a mixed liquid of Nafion solution and water.

The catalyst-coated electrode is first wetted with an electrolyte solution to have no bubbles on its surface. After the electrode is mounted, adjust the distance between the electrode surface and the Lujin capillary (about 2 times the diameter of the Lujin capillary), and try to rotate the electrode two to three times to remove the air bubbles on the electrode surface. The potentiostat was turned on, stabilized at 1600 rpm, and activated at 50–200 $mV.s^{-1}$, and activated until a stable curve was obtained.

3.3.3 Effect of Electrolyte Concentration on the Measurement of Oxygen Reduction Performance of Pt/C Catalyst

At present, most research teams use the rotating ring-disk electrode (RRDE) to study the hydrogenation and oxygen reduction performance of the catalyst. The advantage of this test method is that it can deduct the effect of mass transfer on the measured current, thus reflecting intrinsic properties of the catalyst. In order to ultimately compare the results of RRDE with actual fuel cell membrane electrode (MEA) testing, factors affecting RRDE test results and activity characterization need to be noted. These factors include the determination of the active area, the effects of ion adsorption, the mass transfer effects of the Nafion membrane, and the effects of electrolytes. The first three factors have been studied accordingly. However, in the treatment of electrolytes, it is most commonly used to measure the resistance of the solution by AC impedance method, or to think that the solution is completely conductive, and the solution resistance is negligible. From an electrochemical point of view, the ionic strength of the electrolyte solution will greatly affect the results of the oxygen reduction test. The easiest way to reduce the resistance of the solution and increase the conductance of the solution is to add a certain concentration of strong electrolyte to the solution to increase the number of conductive ions per unit volume of solution. In the study of this book, try to introduce different concentrations of strong electrolyte salt sodium perchlorate in 0.1 M $HClO_4$ to reduce the solution resistance, and study its effect on the oxygen reduction performance of commercial Pt/C catalyst under the oxygen reduction standard test.

3.3.3.1 Electrochemical Characterization

Figure 3.6 is a cyclic voltammetric scan of a commercial Pt/C catalyst in different electrolyte solutions. It can be seen that the addition of different concentrations of

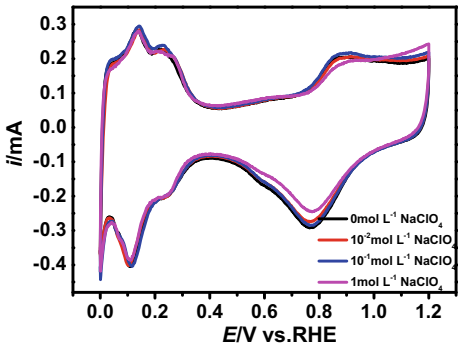

Fig. 3.6 Cyclic voltammetry scan of a commercial Pt/C catalyst in different concentrations of electrolyte solution

sodium perchlorate in 0.1 mol·L^{-1} $HClO_4$ does not affect the potential of hydrogen underpotential precipitation. Moreover, the addition of different concentrations of sodium perchlorate does not affect the peak, peak current and peak area of hydrogen absorption and desorption, indicating that the adsorption of perchlorate on the Pt active point does not increase with the increase of perchlorate ion concentration. Therefore, it is feasible to understand the effect of solution resistance on the oxygen reduction performance of commercial Pt/C catalyst by adding sodium perchlorate. However, the redox peak potential and current density of oxygen are affected by the concentration of the added salt, indicating that the addition of different concentrations of sodium perchlorate will affect the cathodic reduction activity of Pt, and the oxygen reduction reaction is still the rate-determining step of the cathodic reaction.

3.3.3.2 Analysis of Oxygen Reduction Performance

Figure 3.7 is a graph showing the effect of 0.1 M $HClO_4$ solution with different concentrations of sodium perchlorate on the oxygen reduction performance of commercial Pt/C catalysts. It can be seen from Fig. 3.6a that as the concentration of the added salt increases, the measured current density value of the disk electrode at 0.9 V decreases in turn, when the concentration of sodium perchlorate added reaches 1 mol·L^{-1}. The peak potential of the oxygen reduction curve is significantly negatively shifted to 30 mV. In addition, between 0.7 and 0.9 V, the ring current also increases as the concentration of the added salt increases. From the oxygen reduction electron transfer number n and the hydrogen peroxide production amount in Fig. 3.7b, c, it can be seen that in the 0.7–0.9 V region, as the sodium perchlorate concentration increases, the oxygen reduction electron transfer number n decreases. The amount of hydrogen peroxide produced increases. It can be concluded that the addition of sodium perchlorate in 0.1 mol·L^{-1} $HClO_4$ solution has a significant effect on the oxygen reduction performance of commercial Pt/C catalysts, and the cathode reduction of oxygen increases with the concentration of sodium perchlorate added. The reaction became difficult, especially in the electrolyte solution to which 1 mol·L^{-1} $NaClO_4$ was added, the four-electron reduction reaction of partial

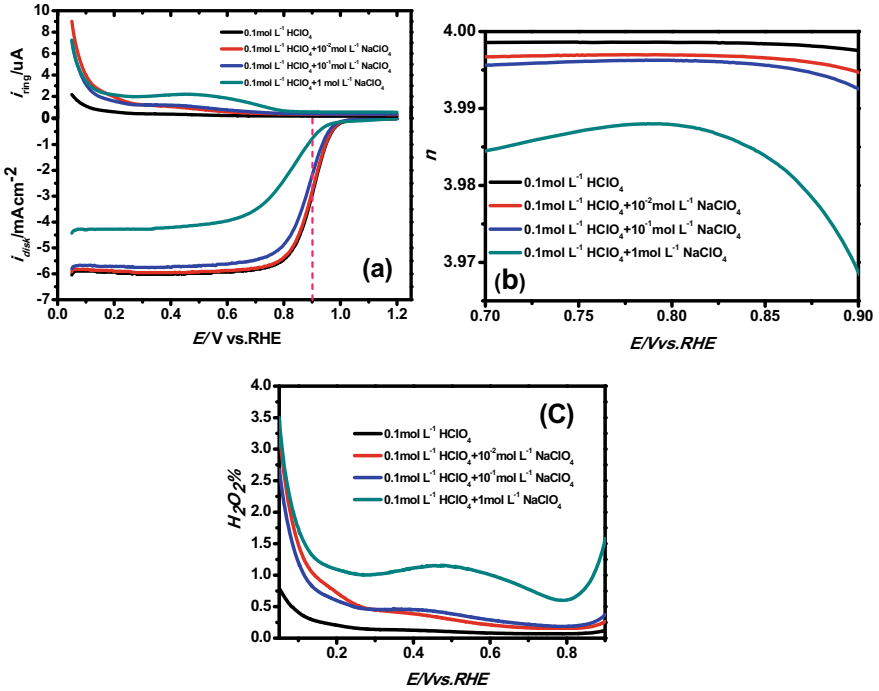

Fig. 3.7 Effect of acidic electrolyte solutions with different concentrations of sodium perchlorate on the oxygen reduction performance of commercial Pt/C catalysts (47.6% Pt, TKK, Japan). **a** Oxygen reduction curve, **b** Number of transferred electrons, and **c** Amount of hydrogen peroxide generation

oxygen was suppressed, and the oxygen reduction performance of the commercial Pt/C catalyst was the worst.

In addition, the value of the limiting current density of the disk electrode in Fig. 3.7a decreases as the concentration of sodium perchlorate added increases. According to the Levich Limit Current Density equation (as shown in Eq. (3.43)), factors affecting the limiting current density are aerobic solubility, electrode speed, temperature, and dynamic viscosity of the solution. It can be seen from Table 3.2

Table 3.2 Concentration of saturated dissolved oxygen in acidic electrolyte solutions with different sodium perchlorate concentrations (25 °C)

Electrolyte solutions	Concentration of saturated dissolved oxygen ($mg.L^{-1}$)
0.1 mol L^{-1} $HClO_4$	20.17
0.1 mol L^{-1} $HClO_4$ + 10^{-2} mol L^{-1} $NaClO_4$	20.25
0.1 mol L^{-1} $HClO_4$ + 10^{-1} mol L^{-1} $NaClO_4$	20.19
0.1 mol L^{-1} $HClO_4$ + 1 mol L^{-1} $NaClO_4$	20.25

that the addition of different concentrations of $NaClO_4$ to 0.1 mol·L^{-1} $HClO_4$ has little effect on the concentration of saturated dissolved oxygen at 25 °C. Therefore, in the case of a certain speed and temperature, the possible cause of the decrease in the limit current density is that the dynamic viscosity of the solution increases as the salt concentration increases, resulting in a decrease in the limit current density value.

$$i_d = 0.62nFD_0^{2/3}\omega^{1/2}v^{-1/6}C_0 \tag{3.43}$$

where ω is the angular velocity, v is the dynamic viscosity ($cm^2.s^{-1}$), C_0 is the concentration (mol·L^{-1}), and D_0 is the diffusion coefficient ($cm.s^{-1}$).

3.3.3.3 Analysis of Oxygen Reduction Activity

Figure 3.8 is a graph showing the effect of a 0.1 M $HClO_4$ electrolyte solution with different concentrations of sodium perchlorate on the kinetic current (a) and mass activity (b) of a commercial Pt/C catalyst. As can be seen from Fig. 3.8, the addition of low concentrations of sodium perchlorate does not have a large effect on its kinetic current and mass activity, and at 0.9 V as the concentration of sodium perchlorate added increases. The kinetic current and mass activity test values were significantly reduced, especially when the sodium perchlorate added was 1 M, the kinetic current and mass activity were minimal, and the mass activity of the commercial Pt/C catalyst was measured at this time. Only 17% of the 0.1 mol·L^{-1} $HClO_4$ solution without salt indicates that the reduction reaction of oxygen at the active point of the catalyst becomes difficult, which is consistent with the deterioration of the oxygen reduction performance of the catalyst in the high concentration salt in the previous part. The 4 electron process was suppressed, making the tested catalyst activity worse.

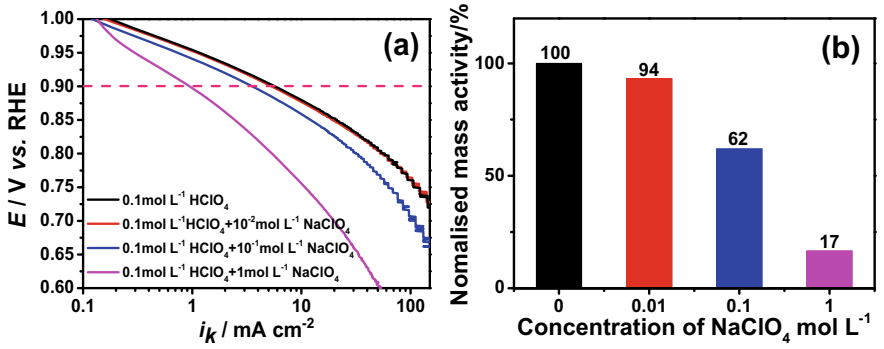

Fig. 3.8 Effect of different sodium perchlorate concentrations of acidic electrolyte solution on mass activity and kinetic current of commercial Pt/C catalysts (47.6% Pt, TKK, Japan). **a** Kinetic current curve and **b** Normalized mass activity

The results showed that different concentrations of sodium perchlorate were added to 0.1 mol·L^{-1} $HClO_4$, and the oxygen reduction mass activity of the commercial Pt/C catalyst was worse than that without time. Moreover, when the concentration of sodium perchlorate added was 1 mol·L^{-1}. The oxygen reduction of the commercial Pt/C catalyst has a negative shift of about 30 mV, and the kinetics of oxygen reduction was hindered. It is indicated that reducing the resistance of the solution by introducing a strong electrolyte salt will affect the test results, and the high concentration of salt will hinder the correct characterization of the oxygen reduction performance of the catalyst. The current possible explanation is that increasing the concentration of salt actually increases the concentration of ions. On the one hand, these ions affect the mass transfer of oxygen on the one hand, and may adsorb on the surface of the electrode on the other hand, affecting the adsorption and reduction of oxygen, and finally, the data that led to the measurement of oxygen reduction performance deteriorated, which is why the conventional oxygen reduction test was carried out in 0.1 mol·L^{-1} $HClO_4$. The following section will discuss in detail the other important factors affecting the oxygen reduction test.

3.3.4 Electrode Film-Forming Technology

In the rotating disk electrode test, the film formation quality and film formation uniformity of the electrode will greatly affect the oxygen reduction activity of the catalyst.

There are two ways to dry the catalyst film. One is the static drying method, that is, the dispersed catalyst slurry is dropped on the surface of the electrode, and then dried in the air or by other auxiliary drying means in a static state, thereby rotating the circle. A uniform film is obtained on the surface of the disk electrode; the other method is a spin-drying method, that is, the dispersed catalyst slurry is dropped on the surface of the electrode, and then the electrode is dried at a certain rotation speed to obtain a catalyst with uniform adhesion film.

3.3.4.1 Static Drying Method

Figure 3.9 is a catalyst film obtained by a static drying method, here taking 19.7% of a Pt/C catalyst as an example (E-TECK). It can be seen from the figure that the catalyst film obtained by the static drying method has the following problems: (1) the film-forming quality of the edge portion of the catalyst film is relatively uniform, and the film quality of the intermediate portion is poor; (2) the center of the electrode is formed. The film thickness is thin, and the edge portion is not completely formed, and the electrode is not completely covered; (3) the film-forming quality of the electrode surface is uniform, but the edge portion is preferentially dried due to faster diffusion, and the center portion of the electrode is finally dried, if when the obtained catalyst

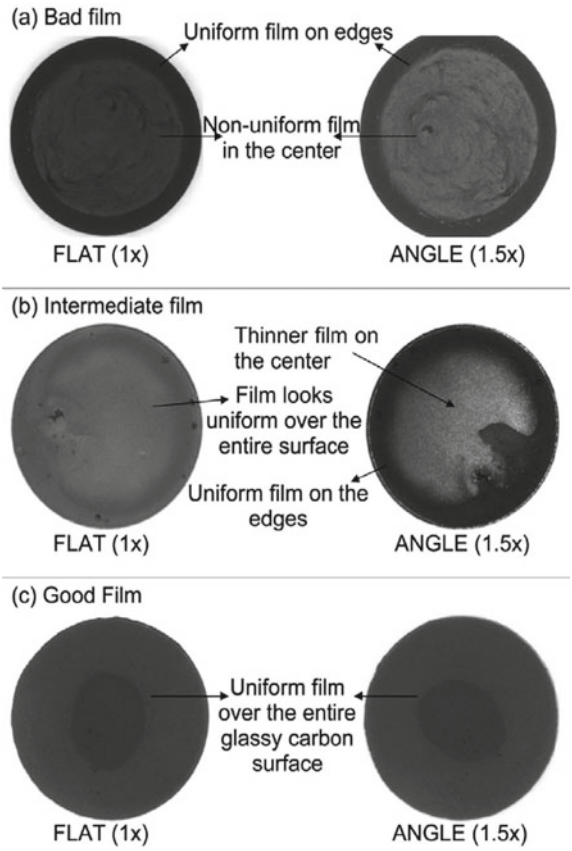

Fig. 3.9 Catalyst film obtained by static drying method. Reprinted from ref. [17], copyright©2010 American Chemical Society, with permission from American Chemical Society

slurry is dispersed very uniformly, it is possible to obtain a catalyst film having a relatively uniform surface dispersion state.

Figure 3.10a is a CV curve of a Pt/C catalyst of different film-forming qualities. It can be seen from the figure that due to the difference in film formation quality, the CV curves obtained by the same catalyst under the same test conditions are greatly different. Whether it is the size of the absorption and desorption peak of hydrogen or the formation position of Pt–OH, the difference is different. As can be seen from Fig. 3.10b, the oxygen reduction polarization curves are quite different. For electrodes with better film formation quality, the slope of the polarization region is larger. In the diffusion control region, the electrode with better film formation quality can obtain a larger limiting current. This is because the electrode with good film formation quality is more conducive to the uniform diffusion of oxygen and electrolyte on its surface.

It can be seen from Fig. 3.11 that the catalyst film obtained by the static drying method has better film formation uniformity at the edge portion, and the thickness of the central portion is significantly thicker, and some central regions are not completely

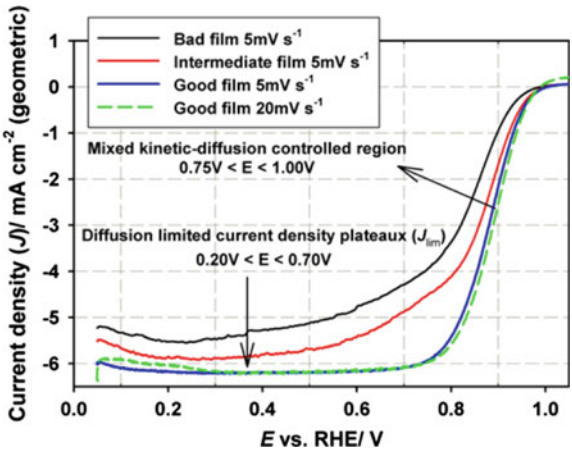

Fig. 3.10 Cyclic voltammogram of the Pt/C catalyst with different filming qualities in 0.1 M $HClO_4$ solution (left) and oxygen reduction polarization curve (right). Reprinted from ref. [17], copyright©2010American Chemical Society., with permission from American Chemical Society

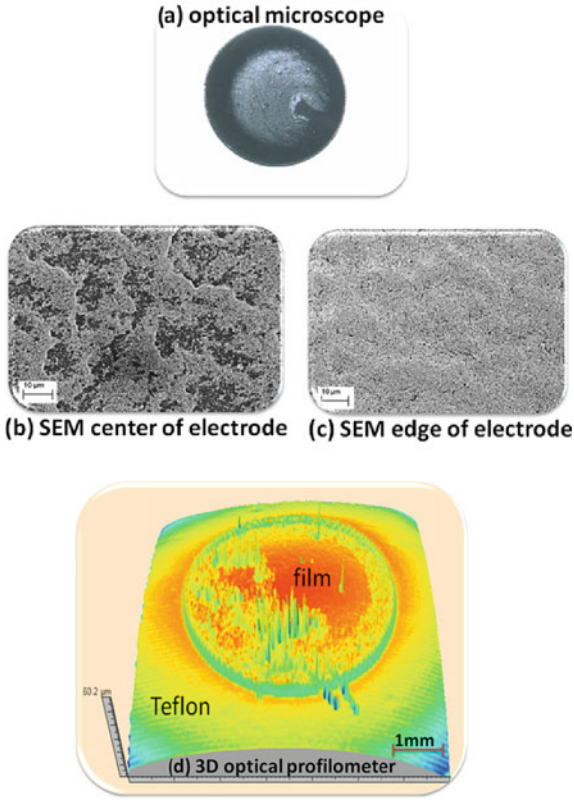

Fig. 3.11 **a** Catalyst film under an optical microscope. **b** SEM photograph of the center of the electrode. **c** SEM photograph of the edge of the electrode. **d** 3D optical photograph of the catalyst film. Reprinted from ref. [18], copyright©2011 Elsevier B.V., with permission from Elsevier

covered, which will affect the electrochemical active area of the catalyst and the magnitude of the oxygen reduction limit current. In addition, since the calculation of the electrochemical active area and the oxygen reduction mass activity is calculated based on the geometrical area of the electrode, it is assumed here that the catalyst film uniformly covers the surface of the electrode, and the actual situation is that the catalyst film obtained by the static drying method is It is not uniform coverage, so the calculation results of the electrochemical active area and the oxygen reduction mass activity are more deviated than the actual values.

3.3.4.2 Rotary Drying Method

In view of the problem of uneven film formation quality in the static drying method, Garsany et al. developed a spin-drying method [18, 19]. The specific method of operation is to invert the rotating disk device, and the electrode on which the catalyst slurry is dropped is turned upward to be rotated to obtain a dried catalyst film. The speed of rotation will cause the catalyst slurry to splash out of the rotating disk electrode. If the rotation speed is too slow, it will not be uniformly dried, and the rotation speed is generally controlled at 700 rpm.

It can be seen from Fig. 3.12 that the film formed by the spin-drying method has a good film-forming quality, and the film-forming quality is relatively uniform regardless of the center of the rotating disk electrode or the edge portion. This is because under the conditions of spin drying, the catalyst slurry can be evenly spread on the surface of the rotating disk electrode, which is more favorable for the solvent in the catalyst slurry to be uniformly volatilized.

It can be seen from Fig. 3.13 that the electrochemical activity areas of the catalysts obtained by the static drying method and the rotary drying method are relatively uniform, but the oxygen reduction activities are quite different. This is because the catalyst film obtained by the spin-drying method is relatively uniform, and thus the electrode is less affected by the surface effect, which is more advantageous for the electrolyte and oxygen to diffuse on the surface of the catalyst. Moreover, the spin-drying method is more reproducible (see Fig. 3.14) and is therefore more suitable for studying the electrocatalytic activity of the catalyst.

3.4 Oxygen Reduction Reaction Test Considerations

The factors that need to be noted during the test are as follows.

The effect of different anions. Markovic et al. found that the reduction of oxygen is greatly inhibited in sulfur- and chlorine-containing acidic electrolyte solutions, which is more pronounced in chlorine-containing electrolyte solutions. Schmidt et al. found that the presence of Cl^- in the electrolyte solution does not change the decisive step of the cathode reduction reaction of commercial Pt/C catalysts, but the

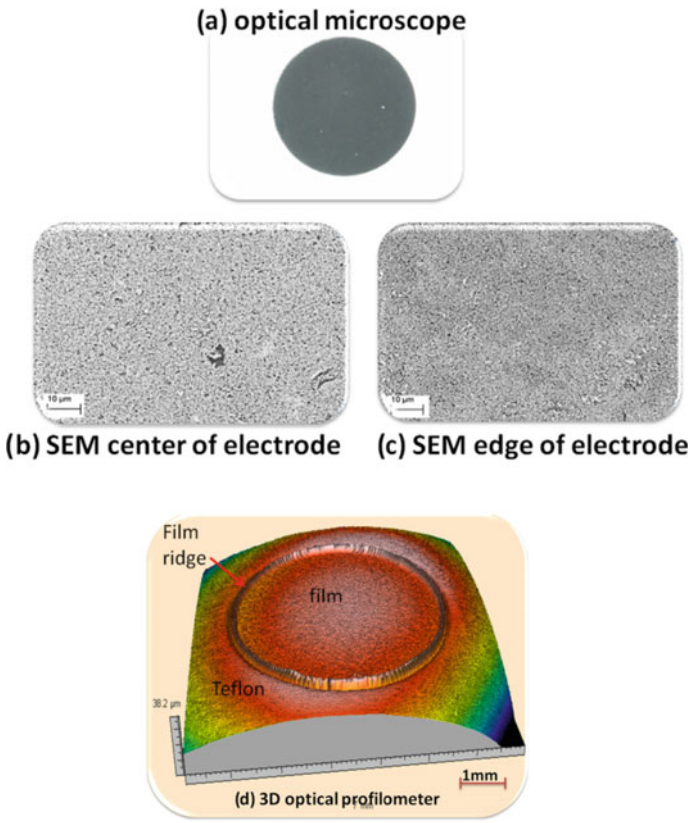

Fig. 3.12 **a** Catalyst film under an optical microscope. **b** SEM photograph of the center portion of the electrode, **c** SEM photograph of the edge of the electrode, **d** 3D optical photograph of the catalyst film. Reprinted from ref. [18], copyright©2011 Elsevier B.V., with permission from Elsevier

formation of H_2O_2 is at the electrode potential >0.2 V, with Cl^- in the $HClO_4$ solution. As the concentration increases, the four-electron reaction process of oxygen is significantly suppressed. We also studied it using polycrystalline Pt disk electrodes. The polycrystalline Pt disk electrode has high activity, low electrode resistance, and is very sensitive to impurities in the solution. It can be used to test the effect of ions on the oxygen reduction reaction in the solution, and more objective results can be obtained. From the practical point of view, we studied the oxygen reduction performance of commercial Pt/C catalysts (Japan TKK, 47.6% Pt) in different acidic electrolyte solutions. The results show that the oxygen reduction performance of commercial Pt/C catalysts is strongly dependent on the type of electrolyte solution. The results show that the oxygen reduction performance of commercial Pt/C catalysts is strongly dependent on the type of electrolyte solution. The oxygen reduction performance of commercial Pt/C catalysts in high concentration acid solutions or in different kinds of inorganic acid solutions is not as good as 0.1 mol·L^{-1} $HClO_4$

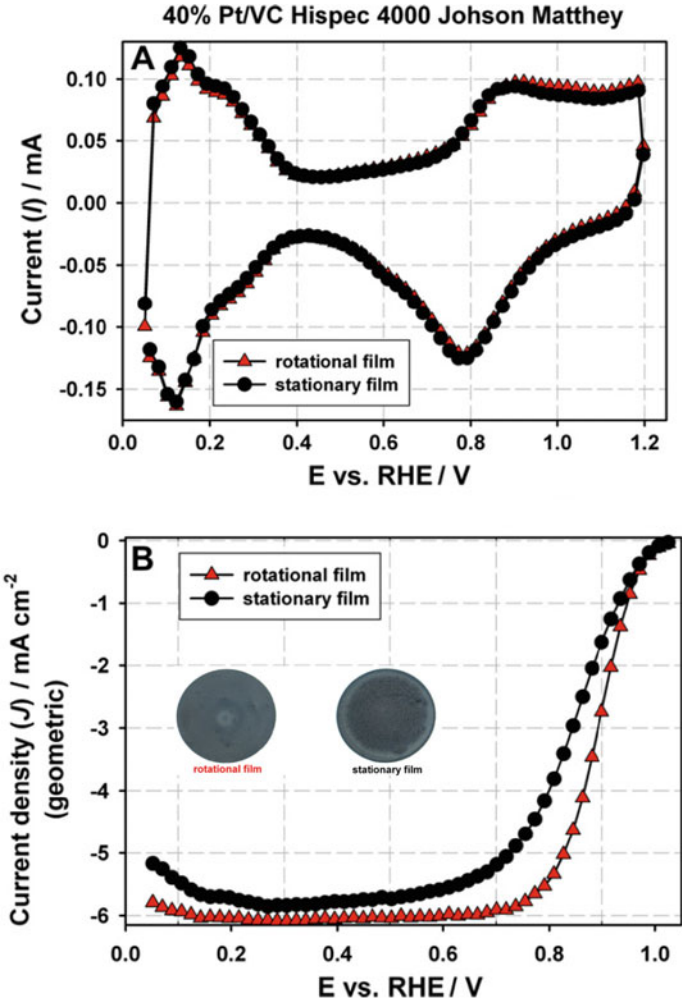

Fig. 3.13 **a** CV curve and **b** oxygen reduction polarization curve of 40% Pt/VC (JM) catalyst obtained by static drying method and spin-drying method, 0.1 M $HClO_4$, 20 mV.s^{-1}, 30°C.Reprinted from ref. [18], copyright©2011 Elsevier B.V., with permission from Elsevier

solution. From Fig. 3.17, we can see that in the solution containing different anionic acids, the oxygen reduction activity ClO_4^- > NO_3^- > SO_4^{2-} > Cl^-, the oxygen reduction overpotential is the largest in the acid solution containing chloride ions. Therefore, during the experimental operation, impurity ions such as Cl^- should be excluded as much as possible. In addition, increasing the ionic strength also reduces the oxygen reduction performance, increases the concentration of sulfuric acid, and deteriorates the performance of oxygen reduction (Fig. 3.15a blue line). Yannick et al. performed oxygen reduction tests on Pt/C catalysts with electrolytes of 0.1 mol·L^{-1}

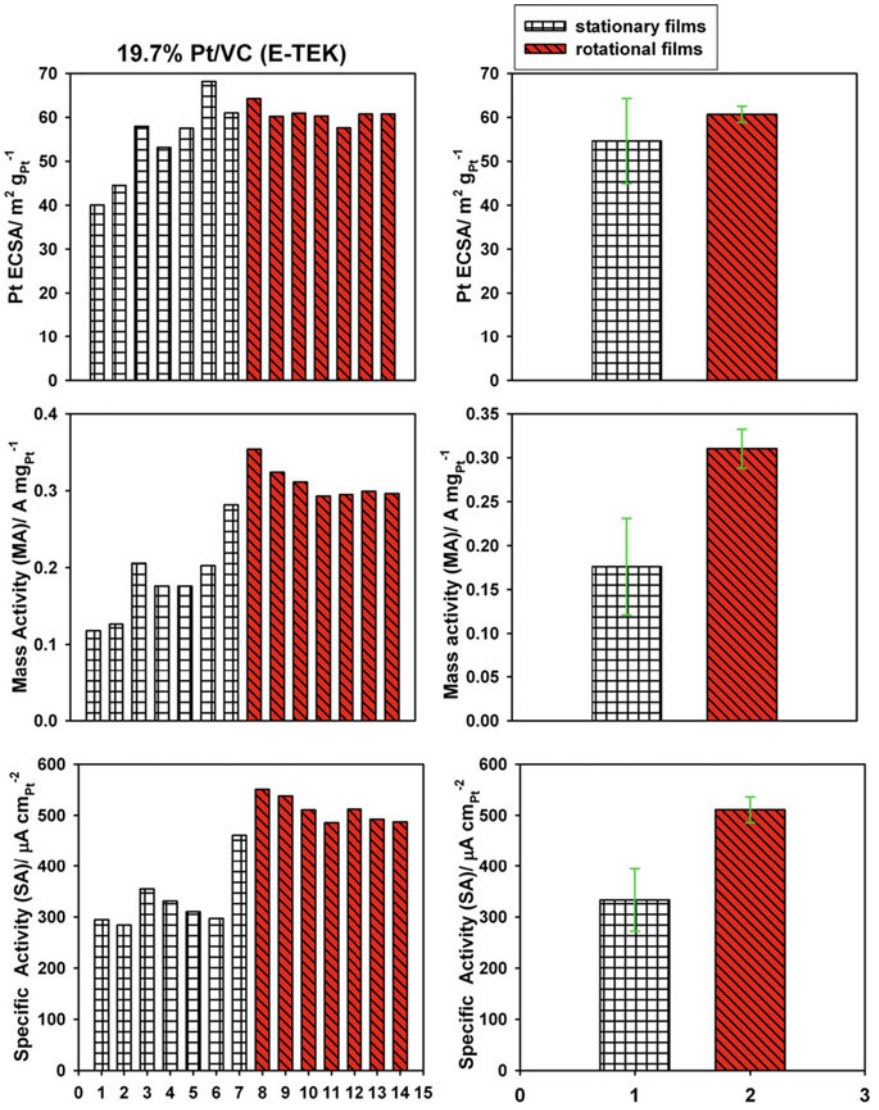

Fig. 3.14 Left: Electrochemical active area and oxygen reduction activity of 40% Pt/VC (JM) catalyst obtained by different drying methods; right panel: difference between electrochemical active area and oxygen reduction activity. Reprinted from ref. [18], copyright©2011 Elsevier B.V., with permission from Elsevier

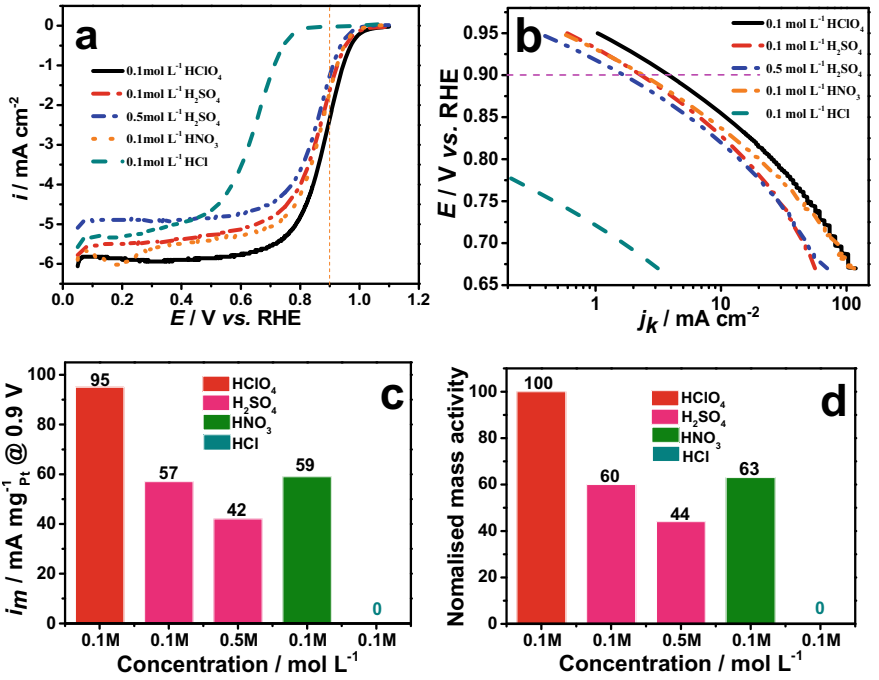

Fig. 3.15 Effect of different acidic electrolyte solutions on the oxygen reduction performance of commercial Pt/C catalysts (Japan TKK, 47.6% Pt). **a** oxygen reduction curve, **b** kinetic current curve, **c** mass activity and **d** normalized mass activity. Oxygen-saturated solution, electrode speed 1600 rpm, potential sweep speed 5 mV.s^{-1}, temperature 25 °C, Pt load 40 μg.cm^{-2}

$HClO_4$, 0.05 mol·L^{-1} H_2SO_4 and 0.5 mol·L^{-1} H_2SO_4 at 1600 rpm and 20 mV.s^{-1}. The results showed that the catalyst had the highest oxygen reduction activity in 0.1 mol·L^{-1} $HClO_4$, and the mass activity in 0.1 mol·L^{-1} $HClO_4$ was 80% higher than that in 0.5 mol·L^{-1} H_2SO_4. In addition, Marković and Schmidt et al. also found that in different electrolyte solutions, oxygen reduced the activity of ClO_4^- > HSO_4^-. Figure 3.15b shows the kinetic current for each catalyst. Based on this result, we can obtain mass activity at 0.9 V (Fig. 3.15c). Based on the activity in 0.1 mol·L^{-1} $HClO_4$, we have a normalized graph comparison (Fig. 3.15d). It can be seen that the commercial Pt/C catalyst is 0.1 mol·L^{-1} H_2SO_4 and 0.5 mol·L^{-1}. The mass activity in the H2SO_4 electrolyte solution was only 60 and 44% in the 0.1 mol·L^{-1} $HClO_4$ solution.

In the choice of electrolyte solution, mainly determined by the performance of the working electrode and the research system, the generally selected electrolyte solution is required to contain no ions that can be adsorbed on the working electrode. For a platinum electrode or a platinum-based catalyst, a perchloric acid solution is an electrolyte solution which does not substantially contain ions which adsorb ions with platinum, and thus is widely used. For most carbon-based materials, whether it

is the use of perchloric acid or sulfuric acid, there is basically no impact on the test. As for the catalyst containing ruthenium, since ruthenium catalyzes the reduction of perchloric acid to form a large amount of strongly adsorbed chloride ions, the electrolyte solution is not suitable for the perchloric acid solution for the oxygen reduction test of the catalyst.

The effect of ionic strength. The commonly used electrolyte solution is a 0.1 mol·L^{-1} $HClO_4$ solution. From an electrochemical point of view, the ionic strength of the electrolyte solution will greatly affect the results of the oxygen reduction test. However, from the literature, our research also found that increasing the concentration of perchloric acid, the performance of oxygen reduction of polycrystalline platinum disk electrode deteriorated. Figure 3.18 shows the results of oxygen reduction of commercial Pt/C catalysts in different perchloric acid concentration solutions. It can be seen that as the concentration of perchloric acid increases (the ionic strength increases), the relative performance of oxygen reduction decreases (Fig. 3.16), and this phenomenon of decreased ionic strength increase performance requires further investigation.

The electrolyte solution used each time should be freshly prepared. An electrolyte solution that is not freshly prepared may have problems. Garsany et al. found that the oxygen reduction performance of the same catalyst in an electrolyte solution used for more than 2 days was significantly worse than that in a freshly prepared electrolyte solution, especially at a low sweep speed of 5 mV.s^{-1}.

The effect of scanning speed. Under the same test conditions, the sweep speed increases, and the limit current increases due to the decrease in the thickness of the effective diffusion layer, which is consistent with the results of the Koutecký-Levich equation.

The test temperature should be constant. The experiment is preferably carried out in a constant temperature water bath, and the change in temperature affects the saturation solubility of the oxygen and the kinetics of the electrode. Although an

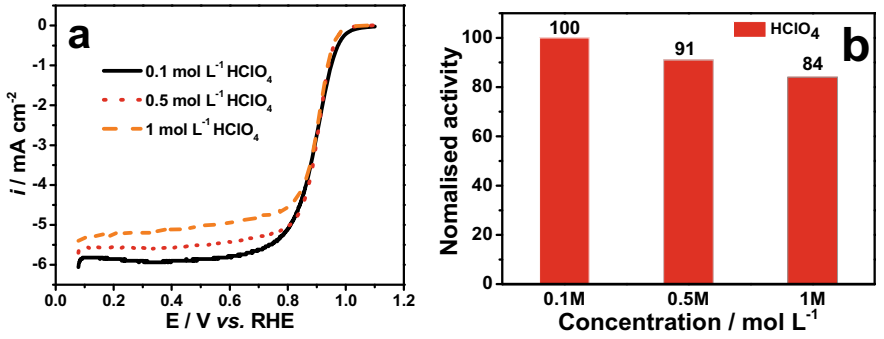

Fig. 3.16 Effect of different concentrations of perchloric acid electrolyte solution on oxygen reduction performance of commercial Pt/C catalyst (Japan TKK, 47.6% Pt). **a** Oxygen reduction curve, **b** Mass activity normalized to 0.1 mol·L^{-1} $HClO_4$ solution. Oxygen-saturated solution, electrode speed 1600 rpm, potential sweep 5 mV.s^{-1}, temperature 25 °C, Pt load 40 μg.cm^{-2}

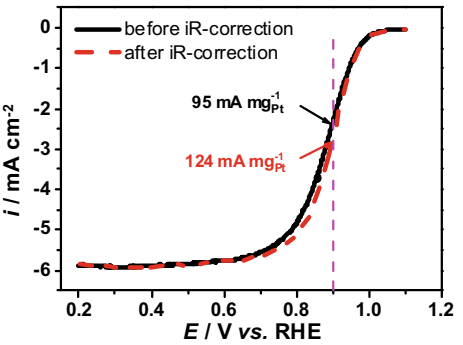

Fig. 3.17 Comparison of the oxygen reduction curve of 47.6% Pt/C commercial catalyst of TKK Company of Japan in 0.1 mol·L^{-1} $HClO_4$ aqueous solution before and after solution resistance correction. Sweep speed 5 mV.s^{-1}, 1600 rpm, 25 °C, platinum loading 40 μg.cm^{-2}

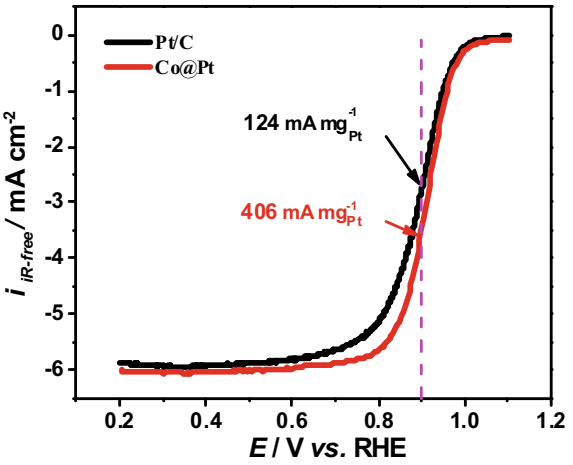

Fig. 3.18 Oxygen reduction curve of 47.6% Pt/C commercial catalyst (black line) and Co@Pt catalyst (red line) of Japan TKK Company in 0.1 mol·L^{-1} $HClO_4$ aqueous solution. The sweep rate is 5 mV.s^{-1}, 1600 rpm, 25 °C, platinum loading, Pt/C 40 μg.cm^{-2}, and Co@Pt 20 μg.cm^{-2}

increase in temperature can improve the kinetics of oxygen reduction, an increase in temperature also reduces the dissolved concentration of oxygen. Therefore, to investigate the effect of temperature on oxygen reduction must take into account the effect of oxygen concentration. Our study found that the oxygen reduction performance measured at 60 °C was not better than the data measured at 25 °C, mainly because the oxygen concentration could not be controlled under normal pressure. Moreover, previous studies have found that at 60 °C, $HClO_4$ will decompose and produce a small amount of chloride ions enough to contaminate the Pt electrode, thus affecting the test results.

The test process should maintain a stable oxygen concentration. Before the experiment, we must pass oxygen for about 30 min, and then measure. Generally, it is necessary to reenergize for about 30 min of oxygen every time to ensure that there is saturated dissolved oxygen in the solution.

The usual conditions for measuring oxygen reduction are the instrument's rotational speed of 1600 rpm, 25 °C, 0.1 mol·L^{-1} $HClO_4$, and a potential sweep rate

of 5 $mV.s^{-1}$. The potential range is set to 0.05 V–1.1 V relative to the reversible hydrogen electrode. The onset potential is determined by the potential of the underpotential hydrogen evolution of the electrode (see next section). The terminal potential is dependent on the initial potential of the oxygen reduction on the electrode. The starting potential of a typical catalyst is around 1 V. If the initial potential of the electrode oxygen reduction is positive, the terminal potential can be increased.

Correction of the oxygen reduction curve solution resistance. The solution resistance has a great influence on the objectivity of the oxygen reduction curve test. If the solution resistance is 10 Ω and the measured current is 1 mA at 0.9 V versus RHE, then the oxygen reduction curve has a 10 mV shift. Although the amount of movement is small, it will calculate the oxygen reduction activity. Have a great impact. Our study found that the mass activity of the commercial Pt/C catalyst after calibration can be increased by about 30%. As can be seen from Fig. 3.17, the change in mass activity values before and after solution resistance correction at 0.9 V versus RHE.

Based on the above measurement conditions, we determined the oxygen reduction curves of commercial Pt/C catalysts and our laboratory-made catalysts (Co@Pt) (Fig. 3.18). The mass activity of the commercial Pt/C catalyst at 0.9 V was 124 $mA.mg^{-1}{}_{Pt}$, and the mass activity of the Co@Pt catalyst was $mA.mg^{-1}{}_{Pt}$.

3.5 Analysis of Electrochemical Reduction Curve of Oxygen

3.5.1 Overview of Electrochemical Reduction Curves of Oxygen

Figure 3.19 shows the oxygen reduction curve sweeped out using the rotating ring disk electrode. The curve consists of an electrochemical polarization region, a concentration polarization region, and a concentration polarization and electrochemical polarization mixing control region, respectively. Electrochemical polarization refers to the phenomenon of electrode polarization caused by the slow reaction of the electrode and the reaction speed of the electrode lags behind the mass transfer rate of the solution. This region is mainly used to analyze the dynamic principle of the working electrode, and to solve the electrode overpotential, exchange current density, etc. Kinetic parameters. Concentration polarization refers to the electrode reaction process, and the diffusion rate of liquid phase mass transfer lags behind the electrode reaction rate, thereby generating electrode polarization. From the concentration polarization region, we can get the limiting current and investigate the factors related to the test conditions through the limiting current.

For concentrated polarization regions, if the cathode electrode reacts to.

$$O + en- \rightarrow R \tag{3.44}$$

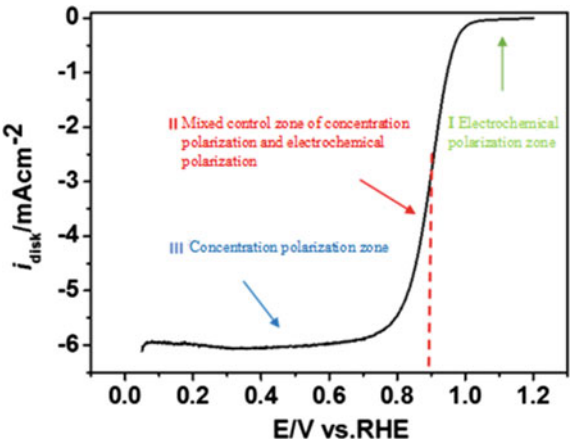

Fig. 3.19 Schematic diagram of the linear volt–ampere curve of oxygen reduction

When the electrode reaction reaches a steady state, according to Fick's first law, the electrode current density can be expressed as follows.

$$i = nFD_0 \frac{a_O^0 - a_O^s}{\delta} \tag{3.45}$$

where $a_o{}^s$ is the activity of substance O on the electrode surface, $a_o{}^0$ is the activity of substance O in the bulk solution, δ is the thickness of the diffusion layer, and D_0 is the diffusion coefficient of substance O.

If the reaction is controlled only by mass transfer (Zone III), the activity of substance O on the electrode surface tends to 0, $a_o{}^s \rightarrow 0$, so the limiting current density can be expressed as follows.

$$i_d = nFD_0 \frac{a_O^0}{\delta} \tag{3.46}$$

For the oxygen reduction reaction, the above formula can be expressed as follows.

$$i_d = \frac{nFD_0C_0}{\delta} \tag{3.47}$$

where D_O is the diffusion coefficient of oxygen and C_0 is the concentration of oxygen in the solution.

It can be seen from the above formula that if the catalyst film is uniform and the thickness is moderate, the limiting current is affected by the temperature, the electrolyte solution and the rotational speed. As the temperature increases, the diffusion coefficient of oxygen molecules increases, but the solubility of oxygen in solution decreases with increasing temperature. Therefore, the effect of temperature on the oxygen reduction limit current is the balance between the two, Paulus et al. The

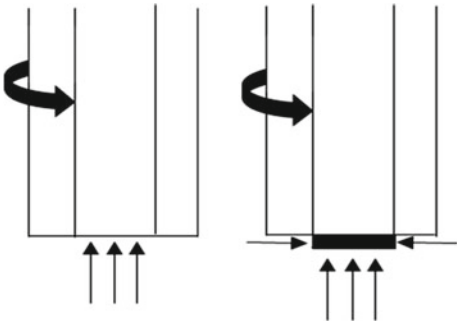

Fig. 3.20 Schematic diagram of the mass transfer effect on the side of the disc electrode film. **a** Thin-film electrode without any side mass transfer; **b** Thick film with side mass transfer

oxygen reduction limit current is the smallest at 80 °C, the maximum at 40 °C, and the limit current at 20 °C is between 80 and 40 °C. In different electrolyte solutions, the diffusion coefficient and solubility of oxygen are different, which affects the value of the limiting current. In addition, as the rotational speed increases, the thickness of the diffusion layer decreases, and the limiting current increases.

For a common thin-film electrode, such as a commercial Pt/C catalyst electrode, the limit current value tends to be 6 $mA.cm^{-2}$ at a sweep rate of 25 °C, 1600 rpm, and 5 $mV.s^{-1}$. For nonplatinum catalysts, the limit current values measured under the same conditions often exceed 6 $mA.cm^{-2}$. This may be because when preparing a nonplatinum catalyst film, the amount of catalyst used in the test tends to be relatively large, and the thickness of the formed catalyst film has exceeded 0.1 μm. At this time, the contribution of side mass transfer to the limiting current of the film electrode is not negligible. Considering the contribution of this part, the limit current value measured under the same conditions will be greater than 6 $mA.cm^{-2}$. The approximate derivation process is as follows (Fig. 3.20).

If the nonplatinum catalyst film layer is uniform, the liquid flow near the electrode is laminar, the catalyst film is simplified to a cylinder, and assuming that the catalyst layer thickness is 0.5 mm and the electrode geometric area A_{geo} is 0.2475 cm^2, the true area of the steady state is involved.

$$\text{Areal} = A_{geo} + A_{side} = 0.2475 + 0.05 * 2 * 3.14 * 0.25 = 0.326\,cm^2 \quad (3.48)$$

According to the Levich limit current equation, at 25 °C, 1600 rpm.

$$i_d = 0.62nFD_0^{2/3}\omega^{1/2}v^{-1/6}C_0 \quad A_{real} = 6 * 0.326 = 1.956\,mA \quad (3.49)$$

$$i_d/A_{geo} = 7.9mA.cm^{-2} \quad (3.50)$$

From the above brief deduction, it is known that the limit current value is amplified in consideration of the influence of side mass transfer. In addition, when the rotating shaft is bent, causing the electrode to sweep through a larger solution area, the phenomenon of limiting current amplification also occurs.

In summary, the limiting current can be used to detect whether the film is uniform, whether the experimental conditions are properly set, and whether the solution is pure.

From the oxygen reduction curve, in addition to the limit current i_d, we can also obtain oxygen reduction parameters such as half-wave potential and initial potential. Thereby, the oxygen reduction performance of the catalyst can be roughly evaluated. Of course, the steeper the oxygen reduction curve, the better the electrical properties of the catalyst.

3.5.2 Mass Activity and Specific Activity

The mass activity i_m (mass activity) and specific activity i_s (specific activity) of the catalyst are two different normalization criteria, that is, the activity is normalized to the active material loading or the active area of the catalyst, so that the objective evaluation can be different. Catalytic activity of the catalyst. Taking metal platinum as an example, its calculation formula is as follows.

$$i_m\ (\text{A mg}_{\text{Pt}}^{-1}) = \frac{i_k\ (\text{mA})}{\text{L}_{\text{Pt}}\ (\mu g)} \tag{3.51}$$

$$i_s\ (\mu A\ \text{cm}_{\text{Pt}}^{-2}) = \frac{i_k\ (\text{A})}{(Q_{H-adsorption}\ (C)/210\ (\mu C\ \text{cm}_{\text{Pt}}^{-2}))} \tag{3.52}$$

where i_k represents the kinetic current, $Q_{H\text{-}adsorption}$ represents the amount of hydrogen absorbed, and L_{Pt} represents the loading of Pt.

It can be seen from the above equation that in order to obtain mass activity and specific activity, it is first necessary to obtain a kinetic current i_k. The kinetic current, also called the net kinetic current, is the current value after removing the mass transfer effect. Below we will derive the kinetic current and further explore how to obtain the kinetic current i_k by correcting the measured current. The derivation process of the kinetic current is as follows.

On the rotating disk electrode, the convection–diffusion equation of the substance j is as shown in (3.57).

$$\frac{\partial C_j}{\partial t} = D_j \nabla^2 C_j - v \nabla C_j \tag{3.53}$$

Among them $\nabla C_j = i\frac{\partial C_j}{\partial x} + j\frac{\partial C_j}{\partial y} + k\frac{\partial C_j}{\partial z}$, D_j is the diffusion coefficient of substance j, the unit is$\text{cm}^2.\text{s}^{-1}$, vector v represents the motion of the solution, and its cylindrical coordinate form can be expressed as follows.

$$v = iu_x + ju_y + ku_z \tag{3.54}$$

Where *i, j, k* are unit vectors, and u_x, u_y, and u_z are the flow rates of the solution in the x, y, and z directions, respectively. In order to solve the convection–diffusion equation of the material on the rotating disk electrode and obtain the concentration distribution of the substance on the surface of the electrode, it is necessary to discuss its velocity distribution *v*. By solving the hydrodynamic Eq. (3.55) under steady-state conditions, Von Karman and Cochran obtained the velocity distribution of the fluid near the rotating disk electrode as shown in Eq. (3.56).

$$\begin{aligned}
&\frac{v_\varphi}{r}\frac{\partial v_r}{\partial \varphi}+v_r\frac{\partial v_r}{\partial r}-\frac{v_\varphi^2}{r}+v_y\frac{\partial v_r}{\partial y}=-\frac{1}{\rho}\frac{\partial \rho}{\partial r}+v(\Delta v_r-\frac{v_r}{r^2}-\frac{2}{r^2}\frac{\partial v_\varphi}{\partial \varphi})\\
&\frac{v_\varphi}{r}\frac{\partial v_\varphi}{\partial \varphi}+v_r\frac{\partial v_\varphi}{\partial r}+\frac{v_r v_\varphi}{r}+v_y\frac{\partial v_\varphi}{\partial y}=-\frac{1}{\rho r}\frac{\partial \rho}{\partial r}+v(\Delta v_\varphi+\frac{2}{r^2}\frac{\partial v_r}{\partial \varphi}-\frac{v_\varphi}{r^2})\\
&\frac{v_\varphi}{r}\frac{\partial v_y}{\partial \varphi}+v_r\frac{\partial v_y}{\partial r}+v_y\frac{\partial v_y}{\partial y}=-\frac{1}{\rho}\frac{\partial \rho}{\partial y}+v\Delta v_y\\
&\frac{1}{r}\frac{\partial v_\varphi}{\partial \varphi}+\frac{\partial v_r}{\partial r}+\frac{v_r}{r}+\frac{\partial v_y}{\partial y}=0
\end{aligned} \tag{3.55}$$

Among them, v_φ, v_r, v_y respectively angular velocity, the linear velocity, and the axial velocity are respectively expressed as follows.

$$\begin{aligned}
v_r &= r\omega(a\gamma-\frac{\gamma^2}{2}-\frac{1}{3}b\gamma^3+..)\\
v_\varphi &= r\omega(1+b\gamma+\frac{1}{3}\alpha\gamma^3+..)\\
v_y &= (\omega v)^{\frac{1}{2}}(-a\gamma^2+\frac{\gamma^3}{3}+\frac{b\gamma^4}{6}..)
\end{aligned} \tag{3.56}$$

Here, a = 0.51023 and b = −0.6159, $\gamma = (\omega/v)^{1/2}y$, ω is the angular velocity of rotation, the unit is s^{-1}, *v* is the kinematic viscosity, the unit is $cm^2.s^{-1}$. The research on rotating disk electrodes is concerned with the speeds v_r and v_y.

Near the surface of the disc, y → 0 (or γ → 0), so

$$\mathrm{vy} = (\omega\mathrm{v})1/2\left(-\alpha\gamma^2\right) = -0.51\omega 3/2\mathrm{v} - 1/2\,\mathrm{y}^2. \tag{3.57}$$

In steady state, the concentration near the electrode is not a function of time, so the convection–diffusion Eq. (3.53) can be written as:

$$v_r\frac{\partial C}{\partial r}+\frac{v_\varphi}{r}\frac{\partial C}{\partial \varphi}+v_y\frac{\partial C}{\partial y}=D_O\left(\frac{\partial^2 C}{\partial y^2}+\frac{\partial^2 C}{\partial r^2}+\frac{1}{r}\frac{\partial^2 C}{\partial r}+\frac{1}{r^2}\frac{\partial^2 C}{\partial \varphi^2}\right) \tag{3.58}$$

Under limiting current conditions, the boundary conditions are:

$$\begin{aligned}
&y=0 \quad C=0\\
&y\to\infty \quad C=C_0
\end{aligned} \tag{3.59}$$

Moreover, C_0 is the concentration of the solution body, regardless of φ, and v_y is independent of r. So (3.58) can be written as:

$$v_y \frac{\partial C}{\partial y} = D_O \frac{\partial^2 C}{\partial y^2} \tag{3.60}$$

Bring (3.57) into (3.60): so

$$\frac{\partial^2 C}{\partial y^2} = \frac{-y^2}{B} \frac{\partial C}{\partial y} \tag{3.61}$$

Among them $B = D_0 \omega^{(-3/2)} v^{(1/2)}/0.51$.

By integrating (3.61) with the upper and lower limits of the integral of (3.60), you can get.

$$C_0 = (\frac{\partial C}{\partial y})_{y=0} (D_0 \omega^{-3/2} v^{1/2}/0.51)^{1/3} \tag{3.62}$$

And because of the current.

$$i = nFAD_0 (\frac{\partial C}{\partial y})_{y=0} \tag{3.63}$$

Here n is the number of electrons involved in the electrode reaction, F is the Faraday constant, and A is the electrode area. So by combining (3.62) and (3.63), you can get the Levich limit current equation.

$$i_d = 0.62nFAD_0^{2/3} \omega^{1/2} v^{-1/6} C_0 \tag{3.64}$$

Under nonlimiting current conditions, only the integral limit of the (3.60)-type integration process needs to be changed.

$$i = 0.62nFAD_0^{2/3} \omega^{1/2} v^{-1/6} \nu C_0 - C_{y=0} \nu \tag{3.65}$$

So $i = i_d \frac{(C_0 - C_{y=0})}{C_0}$ or

$$C_{y=0} = C_0 (1 - \frac{i}{i_d}) \tag{3.66}$$

For a completely irreversible reaction, the disk current can be expressed as:

$$i = FAk_f(E) C_{y=0} \tag{3.67}$$

where $k_f(E) = k^0 \exp\{-af\left(E - E^{\ominus}\right)\}$, $f = F/RT$ k0 is the standard rate constant and α is the transfer coefficient. When there is no exact measurement, α is generally considered to be equal to 0.5.

Substituting (3.66 into (3.67) gives:

$$i = FAk_f(E)C_0(1 - \frac{i}{i_d}) \tag{3.68}$$

Order $i_k = FAk_f(E)C_0$, you can get the Koutecký-Levich equation:

$$\frac{1}{i} = \frac{1}{i_k} + \frac{1}{i_d} \tag{3.69}$$

Where i_k represents the current without any mass transfer, called the kinetic current; i_d is the limiting current; i is the measured current at any potential.

(3.69) can be transformed into:

$$i_k = \frac{i_d \times i}{i_d - i} \tag{3.70}$$

By measuring the oxygen reduction polarization curve, we can obtain the measured current i and the limit current i_d, and substitute it into the above deformation expression to obtain the kinetic current i_k.

After the kinetic current i_k is obtained, the i_k is removed from the mass of the catalyst platinum or its relative electrochemical specific surface area, and two key parameters characterizing the activity of the oxygen reduction catalyst, mass activity im and specific activity is further solved.

The measured current value at 0.9 V versus RHE is generally selected for dynamic correction, and the kinetic current i_k, mass activity i_m and specific activity is calculated. The main reason is that if the important kinetic parameters of the exchange current density are used for correction, since this parameter can only be obtained by extrapolating the measured current, the extrapolation of the extrapolation method causes a large error in the exchange current density, resulting in significant experimental error. In addition, if the activity standard is set at 0.9 V versus RHE, one can guarantee the maximum output of power, because the fuel cell generally operates at less than 0.9 V versus RHE; both can minimize the test error, which is Because at lower potentials, the current is affected by Ohmic drop and oxygen mass transfer, while at higher potentials, the test on the rotating ring disk electrode is affected by the electric double layer, and the fuel cell stack is infiltrated by hydrogen influences. Moreover, the simulation test results of the rotating disk electrode at 0.9 V versus RHE have a high degree of fit with the actual test results of the fuel cell. H. A. Gasteiger et al. reported that the oxygen reduction activity on the rotating disk electrode of the Pt/C catalyst at 0.9 V versus RHE was consistent with that measured by

the fuel cell stack, while at 0.8 V versus RHE there was a bias. Therefore, in combination with various factors, most literature and fuel cell activity standards use 0.9 V versus RHE as the dynamic correction standard and activity comparison standard.

From the above derivation process and the Levich limit current equation, the factors affecting the limit current value include the number of electrons involved in the electrode reaction, the electrode area, the angular velocity of the electrode, the dynamic viscosity of the electrolyte solution, and the diffusion ability and solubility of oxygen molecules. From the current measurement of the limit current in most of the literature, the limit current measured at 1600 rpm for different catalysts is 6 mA.cm^{-2} at 298 K, which also proves that for the speed, temperature, electrolyte type and the oxygen reduction test system of the same concentration has a constant current value as long as the catalyst layer is sufficiently uniform and the thickness is moderate, regardless of the type of the catalyst and the grain size.

If $i_d \rightarrow 6$ mA.cm^{-2}, $L_{Pt} = 20$ μg.cm^{-2}, the relationship between i and i_m can be obtained.

$$i_m(\text{A mg}_{\text{Pt}}^{-1}) \rightarrow \frac{3i(\text{mA cm}^{-2})}{60 - 10i(\text{mA cm}^{-2})} \tag{3.71}$$

The graph of Fig. 3.21 can be obtained by plotting the above formula. When the measured current i at 0.9 V infinitely approaches the limiting current of 6 mA.cm^{-2}, the mass activity i_m increases rapidly.

The mass activity of the catalyst released by the U.S. Department of Energy at 0.9 $V_{iR\text{-free}}$ versus RHE will reach 0.44A.mg$_{Pt}^{-1}$ by 2017. Although most of the current research is focused on improving oxygen reduction activity, there are still many problems to be solved. If only from the point of view of mass activity calculation and oxygen reduction curve analysis, the method of increasing oxygen reduction activity is to increase the measured current of 0.9 $V_{iR\text{-free}}$ versus RHE while ensuring

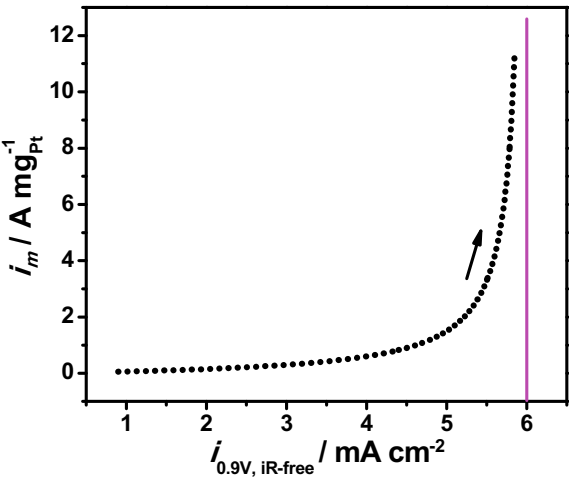

Fig. 3.21 The relationship between i_m and i. $i_d \rightarrow$ 6 mA.cm^{-2}, $L_{Pt} =$ 20 μg.cm^{-2}

the limiting current. From this perspective, the current optimization methods can be simply classified into three categories. The first is to increase the peak potential of oxygen reduction and inhibit the oxidation of Pt. The main methods are Pt-based alloys and ionic liquids. Second, the slope of the curve of the concentration polarization and the electrochemical polarization mixing control region is increased, that is, the internal resistance of the catalyst is lowered or the conductivity of the catalyst is improved. Qu et al. [20] reported that the internal resistance of nitrogen-doped graphene is very small, although the oxygen reduction catalytic activity of this material is still smaller than Pt, especially in the low overpotential region, but it is also a potential material for optimizing oxygen reduction activity. The third method is to reduce the loading of Pt or increase the utilization rate of Pt. The main methods include dealloying, increasing the proportion of Pt(111) crystal plane, increasing the active area, and preparing various special nanostructured catalysts.

Although there are many reports on high-activity oxygen reduction catalysts, Pt-based catalysts are still put into practical use, mainly Pt/C catalysts. The research focuses on the following aspects.

(i) Rotating ring disk electrode test. The effectiveness of the catalyst oxygen reduction still needs further exploration, especially the oxygen reduction simulation test of nonprecious metal catalysts. In many of the literatures already reported, the rotating ring disk electrode test results of most of the new catalysts are highly reproducible and almost identical to actual cell stack test results. However, with the further exploration of catalysts, especially the discovery of nonprecious metal catalysts, it is still unknown whether the rotary ring electrode oxygen reduction simulation test is still valid.
(ii) The relationship between the active substances, the relationship between the carrier and the doping elements, and the activeness of the substances still require more experimental exploration, such as environmental spherical aberration correction electron microscopy and DFT simulation calculations.
(iii) Exploring new forms of catalysts, such as simulated enzyme catalysts, which have lower oxygen reduction over potentials than Pt(111) planes, and even lower than the currently reported Pt_3Ni alloys with the highest activity. It also includes the preparation of self-assembled nanostructured catalysts and the like.
(iv) The high activity catalysts simulated by the simulation should be tested on actual stacks to investigate their activity and stability.
(v) Reduce the cost of an efficient synthetic process for commercialization purposes.

3.6 Electrochemical Determination of Specific Surface Area

The specific activity of the catalyst is required, first of all, to know its electrochemical specific surface area. Ref. [21] details the principle and method of specific surface area measurement. Here we only mention the most commonly used electrochemical test methods.

3.6.1 Overview of Commonly Used Electrochemical Measurements of Specific Surface Area

The electrochemical methods currently used to measure the electrochemical specific surface area of catalysts having a high specific surface area include measuring the integrated charge of the hydrogen desorption zone, the desorption of the saturated adsorbed CO, and the desorption of the underlying potential of the single layer of Cu.

Measuring the desorption amount of saturated adsorbed CO The basic principle of determining the active area is to use CO as a detection molecule, which can occupy all active sites of electrocatalytic activity of the catalyst, and obtain the active area of the catalyst by monitoring the change of the oxidative desorption electric quantity. For organic electrochemical reactions, CO is very easy to achieve CO adsorption because it is an intermediate substance for many reactions. As early as 1962, Gilman began to study the adsorption behavior of CO on the electrode [22], and found that the adsorption of CO is controlled by diffusion and there are at least two bonding states on the polycrystalline platinum electrode. Adsorption of CO can be used to measure the active area of a metal or alloy, but the bonding mode of adsorbed CO is very complicated, such as linear adsorption, bridge adsorption and flat adsorption, and the bonding mode is closely related to metal surface state and defect density. At lower potentials, CO adsorbs strongly on the surface of Pt and other metals. When the adsorption of CO on the surface of the electrode reaches saturated adsorption, it is electrochemically oxidatively desorbed. In this process, oxidative desorption is complete with a single layer of CO. The amount of active point exchanged between the molecule and the electrode is calculated. This part of the oxidative desorption is usually included in the cyclic voltammetry curve, the amount of electricity required for oxidation of the CO, the charge of the electric double layer, the oxidation of the active material, and the oxidation of the remaining adsorbed ions. In the calculation, it is necessary to deduct the electric charge of the electric double layer, the oxidation of the active material, and the oxidation amount of the remaining adsorbed ions, and extract the desorption amount purely for CO oxidation. The electric charge deduction of the electric double layer is generally considered to be the same as that of the electric double layer in the CO oxidation desorption region and the electric double layer region, thereby simplifying the calculation. A more rigorous subtraction method can be found in the literature 23, which proposes two CO double-layer electric charge deduction models, which respectively compare or exclude the influence of the electric quantity caused by the Pt(111) surface special adsorption state on the coverage calculation. The deduction of the oxidative charge of the active material and the remaining adsorbed ions are complicated, which also limits the application of CO in determining the active area. In addition to the complex background current subtraction, the saturated adsorption state of CO is difficult to determine, and there is also a CO coverage problem, such as incomplete coverage or lamination coverage, and measurement results may have large errors. It is generally believed that the

saturation coverage of CO on the Pt electrode is between 0.63 and 0.68 mL, and the power density required for CO oxidation of the single layer of CO is 420 $\mu C.cm^{-2}$.

The basic principle of characterizing the active area by the underpotential deposition of a single layer of Cu is similar to measuring the CO oxidative desorption. Here, the probe atom is Cu, and at the Nernst equilibrium potential, the probe atom begins to deposit on the surface of the substrate. For the catalyst containing metal Ru, the adsorption of CO and H on its surface is accompanied by a large ion adsorption, resulting in a large error, and the adsorption of Cu does not have this problem. However, the main disadvantage of this method is that the metal ions strongly influence the reaction of the catalyst and are not conducive to the cleaning of the electrolytic cell after the reaction.

The electrochemical specific surface area is calculated by the integrated electric quantity of the hydrogen desorption zone. The biggest advantage is that this method is simple and easy and can be directly obtained by integrating the CV curve. In the following, metal platinum is taken as an example to discuss in detail how to calculate the electrochemical specific surface area of the catalyst by measuring the integrated electric quantity in the hydrogen desorption zone and give considerations for using the method.

3.6.2 Integrated Power of Hydrogen Adsorption Zone

Different research teams have different selection tendencies in the choice of hydrogen adsorption or desorption of electricity to characterize the active area. Theoretically, the amount of hydrogen absorbed and desorbed should be the same, but the underpotential reduction of hydrogen easily causes the oxidation of hydrogen, which interferes with the amount of electricity in the hydrogen desorption zone. In addition, setting the upper limit potential of different catalyst oxidation will affect the desorption peak of hydrogen. Considering these factors comprehensively, this paper adopts the method of measuring the electricity in the hydrogen adsorption zone.

For metal Pt, when cyclic scanning is performed in an acidic aqueous solution, a hydrogen atom adsorption peak appears in the potential region of +0.4 ~0.05 V (vs. SHE), and the specific surface area of the electrode can be calculated by the amount of the adsorption peak. As shown in (3.75).

$$\mathrm{ECSA_{Pt}}\ (\mathrm{m}^2\ g_{Pt}^{-1}) = \left(\frac{Q_{H-adsorption}\ (C)}{210\ (\mu C\ cm_{Pt}^{-2}) L_{Pt}\ (mg_{Pt}\ cm^{-2}) A_g\ (cm^2)} \right) \times 10^5 \tag{3.72}$$

Where $Q_{\text{H-adsorption}}$ represents the amount of hydrogen adsorbed, L_{Pt} represents the loading of Pt, and Ag represents the geometric area of the glassy carbon electrode carrying Pt. In the formula, 210 $\mu C.cm^{-2}$ is the electric charge density when Pt

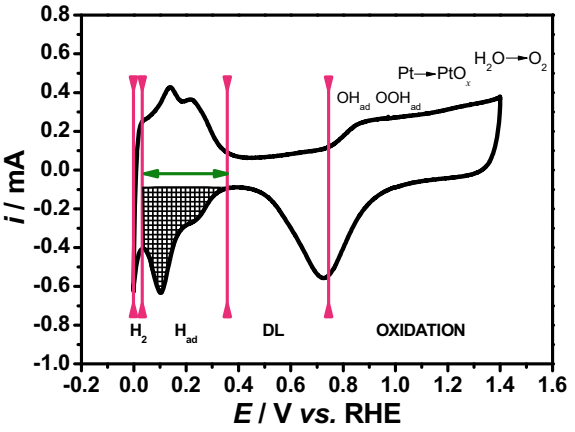

Fig. 3.22 Scanning potential curve of Pt/C electrode in 0.1 mol·L^{-1} $HClO_4$ solution (potential sweep speed 50 mV.s^{-1}. The shaded area is the area of hydrogen adsorption)

is adsorbed on a single layer of H atoms, which is the average value of the three low-index crystal surface charge densities of Pt.

The amount of hydrogen adsorbed by $Q_{H\text{-adsorption}}$ can be obtained by integrating the hydrogen adsorption region on the cyclic voltammetry curve. Figure 3.22 is the cyclic voltammetry curve of a commercial catalyst in 0.1 mol·L^{-1} $HClO_4$ solution. The upper curve of the abscissa in the figure is the forward scan (from low to high) curve, and the lower is the negative scan curve.

The cyclic voltammetry curve can be divided into four different regions. The first region is an underpotential reduction (hydrogen evolution) region (H_{UPD}) of a hydrogen atom. In 1935, Frumkin and Slygin first studied the underpotential reduction of hydrogen on the Pt electrode. In an acidic solution, the oxidation and reduction mechanism of the surface H of the polycrystalline Pt electrode is generally considered to be initiated by the adsorption of H molecules, involving the decomposition of H molecules into adsorbed H atoms and the recombination of H ions into H molecules, which are generally considered to be as follows.

$$H_2 \rightarrow H_{ad} + H_{ad} \tag{3.73}$$

$$H_2 \rightarrow H^+ + H_{ad} + e^- \tag{3.74}$$

$$H_{ad} \leftrightarrow H^+ + e^- \tag{3.75}$$

It can be seen from the above equation that H_{ad} is an intermediate medium for H oxidation or reduction reaction, so the reaction kinetics of H is closely related to the state of H_{ad} on the surface of Pt, that is to say, its coverage has a greater influence on it. The electrode potential varies with the hydrogen atom coverage of the electrode surface $\Theta_{H,\,UPD}$ satisfies the following formula:

$$\frac{\theta_{H,UPD}}{1-\theta_{H,UPD}} = K \exp -(g\theta_{H,UPD}) \times \exp -(EF/RT) \tag{3.76}$$

g is a constant characterizing the two-dimensional lateral growth of the H adsorbed layer.

The underpotential hydrogen evolution process will occur at around 0.05 V depending on the electrode material, not at 0 V. The oxidation of free hydrogen in this process may result in a large desorption of the measured adsorbed hydrogen. Due to the existence of such an underpotential hydrogen evolution process, it is necessary to avoid this region during the oxygen reduction test to avoid the influence of the precipitated hydrogen on the result. This area is typically 0–0.05 V (vs. RHE).

The second region is mainly the absorption and desorption (H_{ad}) of hydrogen, and the amount of electricity passing through this potential region is mainly used to change the amount of hydrogen absorption and desorption.

$$Pt + H_3O^+ + e^- \rightarrow Pt - H_{ad} + H_2O \tag{3.77}$$

If H_{ad} is assumed to be a single layer of adsorption on the surface of a smooth Pt electrode, the amount of hydrogen adsorbed to a single layer of hydrogen is 210 $\mu C.cm^{-2}$. The crystal structure of Pt has a great influence on the precipitation and reduction potential of this region H. The characteristics of the absorption and desorption peaks of hydrogen on different crystal faces are also completely different. On a cyclic voltammogram of 0.5 $mol{\cdot}L^{-1}$ $H2SO_4$solution, for Pt(100), when E < 0.25 V has a larger plateau, E = 0.25 V has a butterfly peak, the latter is in solution The sulfate/hydrogen sulfate ion participates in the adsorption/desorption process. On Pt(111), there are one small and two current spikes at E = 0.1 V and 0.42 V, respectively. The former corresponds to the adsorption of hydrogen on the short-range ordered (111) position, and the latter corresponds to the hydrogen in the long-range order (111) adsorption on the site. On the Pt (110), only the peak at 0.12 V appears. The different adsorption and desorption peaks of hydrogen on the three basic crystal faces have become the criterion for in situ detection of different crystal plane structures.

In the third region, there are few hydrogen atoms adsorbed in the potential range, and the charged electric quantity is mainly used for charging the electric double layer, so it is called "double electric layer region." Since the electric double layer can quickly reach equilibrium, the electric double layer capacitance is independent of the scanning rate and is affected by the electrode potential. The charging current density of the electric double layer can be expressed by the following formula.

$$j_c = C_d \frac{d\varphi}{dt} \tag{3.78}$$

In the formula, C_d is an electric double layer differential capacitance, and $d\phi/dt$ is a rate of change of the electrode potential with time, that is, a scanning rate.

The absorption and desorption of hydroxide and oxygen began to appear in the fourth region. As the potential increases, the adsorbed oxygen atoms and hydroxide ions formed on the surface of the electrode combine with platinum to form oxides (PtO_x) and hydroxides, and even oxygen evolution occurs.

In an acidic solution, Conway et al. believe that at 1.18 V (vs. RHE), the platinum surface is filled with a single layer of PtOH.

$$Pt + H_2O \rightarrow Pt - OH + H_+ + e^- \tag{3.79}$$

Subsequently, PtOH is further reacted to form PtO. Gregory and Jerkewic et al. proposed a potential for forming a single layer of PtO of 1.4 V (vs. RHE).

In an alkaline solution, hydroxide adsorption occurs at about 0.55 V, and the reaction equation is as follows:

$$Pt + OH^- \rightarrow Pt{-}OH + e^- \tag{3.80}$$

PtO is formed at about 0.8 V.

$$Pt{-}OH + OH^- \rightarrow Pt{-}O + H_2O + e^- \tag{3.81}$$

Therefore, this area is called the "oxygen zone." If the reverse phase of the oxygen adsorption zone is reached, as the potential becomes negative, oxygen desorption (reduction), electric double layer charging, and hydrogen adsorption process will occur in sequence.

The hydrogen adsorption zone of the second region is integrated, and the result is the amount of electricity in the zone. Since the region contains the charging of the electric double layer, the result obtained by subtracting this part of the charging power is the hydrogen adsorption amount, and the calculation formula of the adsorption amount of the hydrogen adsorption region is as shown in (3.82).

$$Q_{H-adsorption} = \frac{\int_{E_L}^{E_h} (I - I_{DL}) dE}{v} \tag{3.82}$$

In the above formula,v is the scanning speed, I is the adsorption region current, I_{DL} is the electric double layer charging current, the lower integration limit E_L is the potential at the end of the hydrogen underpotential deposition, generally between 0.03 and 0.05 V, and the upper limit of integration E_h is hydrogen. The end of the adsorption zone determines or the initial potential of the adsorbed hydrogen, typically between 0.45 and 0.5 V.

Taking the shaded portion of Fig. 3.22 as an example, the result is the hydrogen adsorption energy $Q_{H\text{-adsorption}}$, and the hydrogen adsorption energy $Q_{H\text{-adsorption}}$ is substituted into (3.82) to obtain the electrochemical specific surface area. The detailed calculation process is as follows.

$$Q_{H-adsorption} = \frac{\int_{E_L}^{E_h} (I - I_{DL}) dE}{v} = \frac{\int_{0.037}^{0.394} (I + 8.869 \times 10^{-5}) dE}{0.05}$$
$$= 1.52 \times 10^{-3} C \tag{3.83}$$

$$\mathrm{ECSA_{Pt}(m^2\ g_{Pt}^{-1})} = \left(\frac{Q_{H-adsorption}(C)}{210(\mu C\ \mathrm{cm_{Pt}^{-2}}) L_{Pt}(\mathrm{mg_{Pt}\ cm^{-2}}) A_g(\mathrm{cm^2})} \right) \times 10^5$$
$$= \frac{152 \times 10^{-5}}{210 \times 11.9 \times 10^{-3}} \times 10^5$$
$$= 61$$

The catalyst was obtained to have an electrochemical specific surface area of 61 $m^2.g^{-1}$. It should be noted here that since the deduction of the electric quantity of the electric double layer is manual operation, it is recommended to calculate the integral area of the hydrogen adsorption area of three or more CV curves, and take the average value in order to minimize the human error.

Characterization of active regions using electrochemically adsorbed hydrogen species requires attention to the following points:

(i) For most catalysts, the cyclic voltammetry curve is 0–1.4 V versus RHE can generally be divided into four regions. The main difference is the peak current value of each region and the potential of each region. Scope (Fig. 3.16).

(ii) The adsorption capacity of the single layer of hydrogen adsorbed $Q_{H\text{-adsorption}}$ is calculated or tested by the action of the active substance and hydrogen used. The above value of 210 $\mu C.cm^{-2}$ is polycrystalline platinum and three low-index Miller. The average value of the surface hydrogen adsorption amount is the hydrogen adsorption amount which is only considered to be the (100) plane.

(iii) This method is based on the assumption that hydrogen adsorption and its coverage are independent of the surface structure and alloying of the catalyst. However, many studies have found that an increase in the weak bonding mode between hydrogen and the catalyst reduces the amount of hydrogen adsorbed. For example, multilayer adsorption or submonolayer adsorption of hydrogen due to synergy between metals results in a large error in characterizing the electrochemically active area of the platinum-based alloy by hydrogen adsorption. In addition, whether the hydrogen is full of monolayer adsorption at the active site, whether the catalyst and hydrogen are one-to-one adsorption (i.e., pure monolayer adsorption), and the active point contribution of each polycrystalline surface also make the method have greater uncertainty.

(iv) The use of this method requires careful consideration. For example, for a metal-containing Pd catalyst, this method is not suitable because the hydrogen atom not only adsorbs on the metal surface but also penetrates into the gap of the palladium to become a gap atom, that is, palladium absorbs hydrogen atoms. In addition to important metals such as gold, enamel and enamel, this method is not applicable. However, for precious metal ruthenium, measuring the desorption

power of hydrogen to characterize the active area may be the only effective method to characterize the active area of the metal.

In summary, hydrogen desorption and desorption characterizes the active area due to its own premise, which makes it more uncertain, but its operation is simple and can be detected in situ, so it is still a valuable test method.

After obtaining the electrochemical specific surface area, if the net kinetic current i_k is known, the specific activity is further determined. For the activity of the catalyst to be characterized by specific activity, it is necessary to pay attention to the fact that, from the formula, to increase the specific activity, since the increase of the net kinetic current is generally difficult to keep up with the increase of the active area, there are two options, which are greatly reduced. The active area or the net kinetic current is greatly increased. Since the active area can be made very large under normal circumstances, and the increase of the net kinetic current is very small, in many cases, the experimental result is to increase the specific surface area several times, but the specific activity does not increase or even decrease. However, as far as we know, in general, the larger the specific surface area, the higher the utilization rate of the noble metal in the catalyst, and the increase of the specific surface area is advantageous for increasing the utilization rate of the active material of the catalyst and thereby improving the catalytic activity of the oxygen reduction. However, using this activity standard, the most common case is to reduce the active area or the catalyst utilization is beneficial to increase the specific activity, thereby optimizing the oxygen reduction catalytic activity, which is contrary to our research common knowledge. The U.S. Department of Energy has been aware of this problem and has removed the activity standard for activity than the latest DOE indicator.

References

1. Teliska A, O'Grady WE, Ramaker DE (2005) Determination of O and OH adsorption sites and coverage in situ on Pt electrodes from Pt L23 X-ray absorption spectroscopy. J Phys Chem B 109:8076
2. Murthi VS, Urian RC, Mukerjee S (2004) Oxygen reduction kinetics in low and medium temperature acid environment: correlation of water activation and surface properties in supported Pt and Pt alloy electrocatalysts. J Phys Chem B 108:11011
3. Roth C, Benker N, Buhrmester T et al (2005) Determination of O[H] and CO coverage and adsorption sites on PtRu electrodes in an operating PEM fuel cell. J Am Chem Soc 127:14607
4. Teliska M, Murthi VS, Mukerjee S et al (2005) Correlation of water activation, surface properties, and oxygen reduction reactivity of supported Pt–M/C bimetallic electrocatalysts using XAS. J Electrochem Soc 152:A2159
5. Koh S, Leisch J, Toney MF et al (2007) Structure-activity-stability relationships of Pt−Co alloy electrocatalysts in gas-diffusion electrode layers. J Phys Chem C 111:3744
6. Koh S, Toney MF, Strasser P (2007) Activity–stability relationships of ordered and disordered alloy phases of Pt3Co electrocatalysts for the oxygen reduction reaction (ORR). Electrochim Acta 52:2765
7. Yano H, Inukai J, Uchida H et al (2006) Particle-size effect of nanoscale platinum catalysts in oxygen reduction reaction: an electrochemical and 195Pt EC-NMR study. Phys Chem Chem Phys 8:4932

8. Treimer S, Tang A, Johnson DC (2002) A consideration of the application of Koutecký-Levich plots in the diagnoses of charge-transfer mechanisms at rotated disk electrodes. Electroanalysis 14:165
9. Wroblowa HS, Pan YC, Razumney G (1976) Electroreduction of oxygen: A new mechanistic criterion. J Electroanal Chem 69:195
10. Schmidt TJ, Gasteiger HA, Stäbc GD et al (1998) Characterization of high-surface-area electrocatalysts using a rotating disk electrode configuration. J Electrochem Soc 145:2354
11. Lawson DR, Whiteley LD, Martin CR et al (1988) Oxygen reduction at Nafion film-coated platinum electrodes: transport and kinetics. J Electrochem Soc 135:2247
12. Jerkiewicz G, Zolfaghari A (1996) Determination of the energy of the metal-underpotential-deposited hydrogen bond for rhodium electrodes. J Phys Chem 100:8454
13. Zolfaghari A, Jerkiewicz G (1999) Temperature-dependent research on Pt(111) and Pt(100) electrodes in aqueous H_2SO_4. J Electroanal Chem 467:177
14. Xiancai Fu et al (2006) Physical chemistry (Volume II). Higher Education Press, Beijing
15. Liang Y, Li Y, Wang H et al (2011) Co3O4, nanocrystals on graphene as a synergistic catalyst for oxygen reduction reaction. Nat Mater 10:780
16. Li Y, Zhou W, Wang H et al (2012) An oxygen reduction electrocatalyst based on carbon nanotube—nanographene complexes. Nat Nanotech 7:394
17. Garsany Y, Baturina OA, Swider-Lyons KE, Kocha SS (2010) Experimental methods for quantifying the activity of platinum electrocatalysts for the oxygen reduction reaction. Anal Chem 82:6321–6328
18. Garsany Y, Singer IL, Swider-Lyons KE (2011) Impact of film drying procedures on RDE characterization of Pt/VC electrocatalysts. J Electroanal Chem 662:396–406
19. Garsany Y, Ge J, St-Pierre J, Rocheleau R, Swider-Lyons KE (2014) Analytical procedure for accurate comparison of rotating diskelectrode results for the oxygen reduction activity of Pt/C. J Electrochem Soc 161:F628–F640
20. Qu L, Liu Y, Baek JB et al (2010) Nitrogen-Doped graphene as efficient metal-free electrocatalyst for oxygen reduction in fuel cells. ACS Nano 4:1321–1326
21. Chikazawa M, Takei T (2006) Surface characterization of powder particles-surface properties and powder properties. In: Masuda H, Higashitani K, Yoshida H (eds) Powder Technology Handbook, 3rd edn. CRC Press, p 325
22. Gilman S (1962) A study of the adsorption of carbon monoxide and oxygen on platinum significance of the "polarization curve." J Phys Chem 66:2657
23. Orts JM, Fernández-Vega A, Feliu JM et al (1992) Electrochemical behaviour of CO layers formed by solution dosing at open circuit on Pt (111) voltammetric determination of CO coverages at full hydrogen adsorption blocking in various acid media. J Electroana Chem 327:261